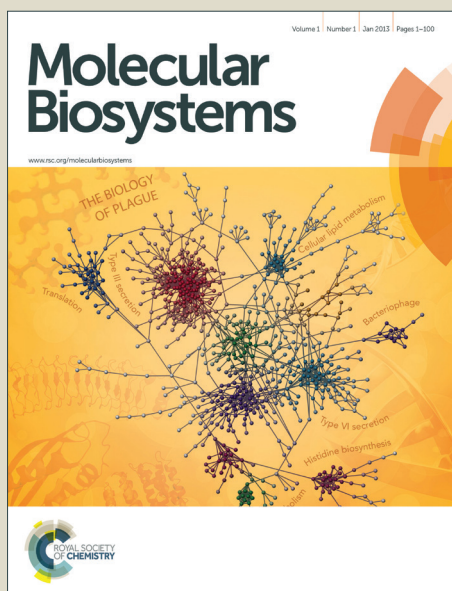


Molecular BioSystems

Accepted Manuscript



This is an *Accepted Manuscript*, which has been through the Royal Society of Chemistry peer review process and has been accepted for publication.

Accepted Manuscripts are published online shortly after acceptance, before technical editing, formatting and proof reading. Using this free service, authors can make their results available to the community, in citable form, before we publish the edited article. We will replace this *Accepted Manuscript* with the edited and formatted *Advance Article* as soon as it is available.

You can find more information about *Accepted Manuscripts* in the [Information for Authors](#).

Please note that technical editing may introduce minor changes to the text and/or graphics, which may alter content. The journal's standard [Terms & Conditions](#) and the [Ethical guidelines](#) still apply. In no event shall the Royal Society of Chemistry be held responsible for any errors or omissions in this *Accepted Manuscript* or any consequences arising from the use of any information it contains.



www.rsc.org/molecularbiosystems

Hyperdiploid tumor cells increase phenotypic heterogeneity within Glioblastoma tumors.

Prudence Donovan¹, Kathleen Cato², Roxane Legaie³, Rupal Jayalath⁴, Gemma Olsson⁴, Bruce Hall⁴, Sarah Olson⁴, Samuel Boros⁵, Brent A. Reynolds⁶, Angus Harding^{2*}

1. Ecole polytechnique fédérale de Lausanne EPFL, School of Life Sciences SV, Swiss Institute for Experimental Cancer Research ISREC, Switzerland.
2. The Translational Research Institute, Princess Alexandra Hospital, Queensland, Australia.
3. QFAB, Queensland Bioscience Precinct, The University of Queensland, Australia.
4. Department of Neurosurgery, Princess Alexandra Hospital, Queensland, Australia.
5. Department of Pathology, Princess Alexandra Hospital, Queensland, Australia.
6. Department of Neurosurgery, University of Florida, Florida, USA.

* To whom correspondence should be addressed

Abstract

Here we report the identification of a proliferative, viable, and hyperdiploid tumor cell subpopulation present within Glioblastoma (GB) patient tumors. Using xenograft tumor models, we demonstrate that hyperdiploid cell populations are maintained in xenograft tumors and that clonally expanded hyperdiploid cells support tumor formation and progression in vivo. In some patient tumorsphere lines, hyperdiploidy is maintained during long-term culture and in vivo within xenograft tumor models, suggesting that hyperdiploidy can be a stable cell state. In other patient lines hyperdiploid cells display genetic drift in vitro and in vivo, suggesting that in these patients hyperdiploidy is a transient cell state that generates novel phenotypes, potentially facilitating rapid tumor evolution. We show that the hyperdiploid cells are resistant to conventional therapy, in part due to infrequent cell division due to a delay in the G_0/G_1 phase of the cell cycle. Hyperdiploid tumor cells are significantly larger and more metabolically active than euploid cancer cells, and this correlates to an increased sensitivity to the effects of glycolysis inhibition. Together these data identify GB hyperdiploid tumor cells as a potentially important subpopulation of cells that are well positioned to contribute to tumor evolution and disease recurrence in adult brain cancer patients, and suggest tumor metabolism as a promising point of therapeutic intervention against this subpopulation.

Introduction

Since Nowell's seminal paper describing cancer as an evolutionary system ¹, many studies have provided compelling evidence supporting the hypothesis that tumor heterogeneity drives the evolution of therapy resistance in cancer patients (reviewed in ²⁻⁸). In this paradigm, individual cancer cells are the reproductive units within a tumor ¹. Those cells that acquire a survival advantage through random genetic or heritable epigenetic change are selected through multiple rounds of clonal expansion, during which they can acquire further alterations that eventually combine to produce malignant phenotypes ¹. The ability of a tumor to evolve is a function of the heritable variation present within the tumor before the application of a selection pressure such as therapy ²⁻⁸. For example, in lung cancer and leukemia, clones with point mutations within oncogenic receptor tyrosine kinases drives tumor recurrence that is resistant to further therapy ⁹⁻¹¹, and resistant mutants have been found in patient tumors before drug treatment ¹². These and other studies show that therapies can select for resistant mutants from the genetically diverse clones already present within the tumor ²⁻⁸. The presence of extensive genetic and

epigenetic heterogeneity enhances the adaptive capacity of tumors by increasing both the frequency and the diversity of therapy resistant tumor cells, and heterogeneity remains a fundamental obstacle preventing the development of curative treatments for many high-grade cancers²⁻⁸.

One example of a solid malignancy with high heterogeneity and poor long-term survival is Glioblastoma (GB), the most common primary malignancy of the central nervous system in adults¹³. Current treatment for GB combines maximal surgical resection^{14, 15} followed by fractionated radiotherapy¹⁶ and concomitant temozolomide¹⁷. Although this therapeutic regime has resulted in improved survival time for GB patients^{18, 19} it remains an incurable disease, with median survival times of 9-15 months despite the combination of aggressive surgery, radiation and temozolomide therapies¹⁸⁻²⁰. Evidence suggests it is the presence of therapy-resistant GB tumor cells that drives the initiation of tumor re-growth after therapy, as revealed clinically in two ways. First, recurrent tumors generally develop within 1-2 centimeters of the resection cavity in tissue that has received intensive cytotoxic therapy²¹; second, recurrent tumors are usually highly refractory to further radiation therapy and chemotherapy²².

A striking feature of GB is the high degree of genomic heterogeneity present within patient tumors (reviewed in²³). Early studies revealed the presence of significant karyotypic variability among GB cells isolated from patient tumors²⁴ and established GB cell lines²⁵, and this karyotypic heterogeneity correlates with phenotypic variation as assessed by the variable expression of antigenic markers²⁵, and more recently through the heterogeneous expression of receptor tyrosine kinases^{26, 27}. Karyotypic variability within patient tumors was confirmed by cytogenetic analyses showing regions of chromosomal aberrations within patient tumors^{28, 29} as well as a high prevalence of aneuploidy³⁰ and intra-tumor chromosomal imbalance³¹ present throughout patient tumors. Genomic heterogeneity correlates with functional heterogeneity in GB tumor cells, as the *in vivo* phenotypes of GB tumor cells vary greatly with respect to their morphology, growth rates, drug responses, and response to growth factors^{27, 32}. Importantly, a variety of clones isolated from a single GB tumor displayed a wide range of sensitivity to chemotherapies, revealing there exists a heterogeneous response to therapy within patient tumors³² that is likely to facilitate the evolution of therapy resistance in patients².

The potential mechanisms underpinning GB resistance to conventional therapy are diverse. Radio-resistance can be mediated by microRNA expression³³, receptor tyrosine kinase amplification and activation³⁴⁻³⁶, activation of signal transduction pathways³⁷⁻⁴¹, nuclear erythroid-related-factor-2 expression (Nrf2)⁴², enhanced DNA repair and homologous recombination^{22, 43, 44}, hypoxia and tumor

microenvironments⁴⁵⁻⁴⁷, and expression of heat shock proteins^{48, 49}. Temozolomide (TMZ) is converted to its active metabolite 5-(3-methyltriazene-1-yl) imidazole-4-carboxamide (MTIC) at physiological pH⁵⁰, which reacts with DNA, forming a wide range of DNA damage adducts that cause DNA strand breaks and cell death⁵¹. There are several DNA repair mechanisms that can be modified by GB cells to allow survival of TMZ treatment⁵². Of particular relevance to acquired TMZ resistance is the DNA mismatch repair system. TMZ DNA adducts function as miscoding bases during DNA replication. These miscoding bases are recognized by the DNA mismatch repair system (MMR) system, which triggers a futile DNA repair process that causes DNA strand breakage and cell death. MMR proteins are prone to inactivation by TMZ-induced mutations^{53, 54} and other mechanisms^{55, 56}, providing GB cells with an escape mechanism from TMZ therapy.

Tumor heterogeneity also fuels tumor adaptation to targeted therapies. One relevant example is the vaccine strategy recently trialed in GB patients, which invoked a patient immune response targeting the truncated, oncogenic EGFRvIII variant of the EGF receptor⁵⁷. The EGFRvIII variant is present in approximately one third of GB patients⁵⁸ and is an ideal target for anti-tumor immunotherapy as the constitutive activity of the EGFRvIII contributes to tumorigenicity, invasion and therapy resistance (reviewed in⁵⁷). Although the vaccine significantly increased overall survival time in treated patients, whose tumors expressed the EGFRvIII receptor, disease recurrence occurred in all patients with 82% of the recurrent tumors losing EGFRvIII expression⁵⁷. EGFRvIII expression is typically heterogeneous in GB tumors, and is only observed in a subpopulation of tumor cells and rarely in the entire tumor^{59, 60}. A plausible hypothesis is that the vaccine led to the immune-clearance of EGFRvIII expressing cells from patient tumors, but the presence of viable EGFRvIII negative cells within the tumor allowed immunological escape and tumor recurrence. As divergent expression patterns in gliomas have been reported for many growth factor receptors^{26, 27, 61-63} as well as other clinically relevant proteins⁶⁴⁻⁶⁷, GB tumor heterogeneity is likely to be an ongoing problem for the development of truly efficacious targeted therapies.

An emerging tumor subpopulation that has been shown to contribute to therapy resistance in a variety of solid tumors are tumor cells that contain elevated levels of genomic DNA (i.e. polyploidy and hyperdiploidy)⁶⁸⁻⁷². Inspired by these studies, we sought to determine whether hyperdiploid cells represent a therapy-resistant subpopulation within GB tumors. We have identified a slow-cycling, tumorigenic hyperdiploid tumor cell population present within GB patients that can initiate and maintain tumor growth *in vivo*, and are resistant to conventional therapy. These results identify a GB hyperdiploid tumor cell subpopulation that has the phenotypic potential to contribute to the evolution of

therapy resistance in patients. Recent work is beginning to identify hyperdiploid-specific drugs⁷³⁻⁷⁷, which may provide a therapeutic opportunity to deplete hyperdiploid cell subpopulations from solid tumors. Here we show that GB hyperdiploid tumor cells are larger and more metabolically active than euploid tumor cells, and that hyperdiploid tumor cells are vulnerable to therapies targeting tumor metabolism. Together, our results support the hypothesis that hyperdiploid tumor cells are a clinically relevant GB tumor cell subpopulation that contributes to the phenotypic heterogeneity that is present within GB patient tumors.

Material and Methods

Tumor sample, primary tumorsphere culturing and propagation

All brain tumor samples used in this study were collected from patients undergoing surgical treatment and were obtained following written informed consent following guidelines established by the Princess Alexandra Hospital Research Ethics Committee, who specifically approved this study (Human Research Ethics Committee reference number HREC/09/QGC/45). Signed consent forms are kept with patient medical records. Biopsies were classified by neuropathologists as Glioblastoma according to WHO guidelines⁷⁸. After surgical removal, the tissue was washed and mechanically dissociated before being placed in an enzymatic cocktail containing Acutase (Sigma) for 10min at 37°C, followed by filtration through a 40-mm filter, and then centrifuged. The cell pellet was then resuspended in red cell lysis buffer (8.3g NH₄Cl, 1.0g KHCO₃, 1.8ml of 5% EDTA in 1000 ml H₂O) and immediately centrifuged. The cell pellet was then resuspended in complete serum-free neurosphere media⁷⁹ and filtered through a 40mm-filter. Cell number was estimated using haemocytometer, dead cells were identified using trypan blue labeling.

Cells were then transferred (at a density of approximately 50,000 viable cells per ml) into neurosphere assay growth conditions⁷⁹. This serum-free culture system containing epidermal growth factor (EGF, 20 ng/ml, R&D) and basic fibroblast growth factor (bFGF, 10 ng/ml, R&D) and enables isolation and expansion in vitro of Glioblastoma tumor cells. Under these culture conditions, the tumor cells generate gliomaspheres that can be serially passaged, as reported by⁸⁰. This technique has proven to preserve the genotype and phenotype of the original tumor compared to traditional serum culture conditions⁸¹, and tumorsphere formation under these culture conditions is an independent prognostic factor for both adult and pediatric brain cancers^{82, 83}.

Briefly, when the tumorspheres have reached an adequate size (~150mm diameter), they were dissociated using enzymatic digestion with Acutase for 3–5 min. Finally, cells were washed, counted using trypan blue to exclude dead cells and replated in fresh media supplemented with epidermal growth factor and basic fibroblast growth factor. We generated the patient-specific human Glioblastoma tumorsphere cultures that we used in the current study. Neonatal Foreskin Fibroblasts (NFF) cells were used as diploid controls, with culture conditions and Human Ethics as described in ⁸⁴.

Isolation of hyperdiploid clones and assessment of long-term proliferation potential

Clonal GB cultures derived from a primary Glioblastoma tumorsphere culture using limiting dilution into 96-well dishes, then each culture derived from a single cell amplified and to derive clonal hyperdiploidy populations from the parent cultures. Single cell cultures were left to divide and expanded into 96 well and 24 well plates. After expansion, these cells were assed for ploidy by flow cytometry (below). Three independent hyperdiploid clonal cultures were then assessed for the potential to maintain long term proliferation cultures at a density of 50 000 cells per ml. Each cell line was sub-cultured at this ratio every seven days over an 11-week period to observe the maintenance of viable, proliferative cultures, growth curves were obtained using the method described in ⁸⁰.

Flow Cytometry

For flow cytometry, single cell suspensions from tumor-spheres, xenograft tumors and primary patient tumors were prepared as described above for long-term culturing. We stained the live cells using Invitrogen LIVE/DEAD® Fixable Cell Stain in the far red channel exactly as described by the manufacturer, and the exactly as described in ⁸⁵, washed the cells twice in cold PBS, then fixed the cells at room temperature with 4% PFA in the dark for 10 minutes. Fixed cells were washed in PBS and then permeabilized for 10 minutes on ice using cold methanol. Cells were either stored at -20°C in methanol or used immediately. For antibody staining, cells were washed once in PBS and then suspended in block buffer (PBS with 1% BSA (Sigma)). Cells were counted, and 1×10^6 cells were stained (antibodies: leukocyte common antigen (LCA) CD45 BD Bioscience Alexa Fluor® 700 Mouse Anti-Human CD45 Catalogue number 560566; neural cell adhesion molecule 1 (NCAM-1) BD Bioscience Alexa Fluor® 647 Mouse Anti-Human CD56 Catalogue number 563443) exactly as described in ⁸⁵. Determination of ploidy by flow cytometry using nucleic acid stains has been shown to be a sensitive and reliable method and is used routinely to asses ploidy levels in cancer cells ⁸⁶. We used DAPI dilactate at a final concentration of 300 nM in PBS. DAPI solution was added to cells at the completion of all other staining immediately before running the sample through the flow cytometer.

To reduce experimental variation between samples due to variations in cell number during staining, we spiked each sample with a primary human diploid control cell population. To identify the control population after data acquisition, live control cells were labeled by staining with carboxyfluorescein diacetate succinimidylester (CFSE) as described in ⁸⁵, then fixed and permeabilized using PFA and methanol as described above. Control, CFSE-stained cells were spiked into test samples, ensuring that the control and test cell populations were exposed to identical staining conditions. We used a Beckman Gallios flow cytometer, and analyzed data using FLOWJO software. A description of our gating strategy is supplied in the supplementary material (Supplementary Figure 1).

To more readily compare genomic content of multiple different tumor lines, we identified the 2n peak for each line and normalized this relative to the diploid control to generate the relative ploidy for each line. Briefly, tumor cell line sample spiked with CFSE-stained normal human diploid control were stained with identifying antibodies as described above as well as for DNA content using DAPI. Appropriate single cell populations were identified using the gating strategy outlined above, and then the 2n DNA peaks for the tumor cells and the normal diploid control were identified and gated on as outlined in the supplementary material (Supplementary Figure 2). The raw flow cytometry data for the 2n peaks was exported as a Txt file from FlowJo and then imported into Prism for analysis. Briefly, the mean fluorescence for the spiked normal diploid control present in each sample was determined using the Prism statistical analysis, and this value was then used to normalize each tumor sample 2n peak using the Prism Normalization function. After normalization relative ploidy was expressed as a fraction, with one representing the normal human diploid DNA content. For convenience we display the normalized 2n cell population data graphically as box plots, which allows a straightforward visual comparison of relative DNA content of the different samples on a single graph.

Drugs response assays using MTT

Proliferation and sensitivity to drugs were assessed using the colorimetric 3-(4,5-dimethylthiazol-2-yl)-2,5-diphenyltetrazolium bromide (MTT) assay as described previously ⁸⁷. Briefly, 5000 cells of each cell line were plated per well in 96-well plates in 100 μ L medium with or without drug. To assess the sensitivity of hyperdiploid clones to Temozolmoide (TMZ, Sigma), TMZ was diluted to final concentration of 60 μ M in 100 μ L of medium. 2-deoxy-D-glucose (2-DG, Sigma) was diluted to a final concentration of 4mM. Cells were allowed to proliferate for 7 days prior to the measurement of cell viability with the addition of 10 μ L MTT (5mg/mL, Sigma) solution to each well and the plate was incubated for 2.5 h at 37°C. Medium was then aspirated from each well, and 100 μ L solubilization

solution (0.1N HCl, 10% TritonX in isopropanol) was added. Colorimetric analysis was performed at a wavelength of 690nm and 570 nm using a standard micro-plate reader. The background absorbance of multi-well plates at 690 nm was subtracted from the 570 nm measurements; the data were plotted in Prism and reported as the mean normalized to vehicle control values. The drug response assays were performed in triplicate for each cell line per assay and with three biological replicates per cell line. The data plotted represent the standard error of the mean from three independent experiments.

Xenotransplantation assay

These procedures were carried out in strict accordance with the National Health and Medical Research Council Guidelines for the care and use of animals for scientific purposes. The protocol was approved by the University of Queensland Animal Ethics Committee (Approval Number UQDI/097/09/NHMRC). We used 6- to 10-week-old female non-obese diabetic/severe combined immunodeficient (NOD/SCID) mice for all surgeries, following institutional and national regulations, exactly as described in ⁸⁵. After tumor cell implantation, the animals were monitored for any neurological signs affecting their quality of life. When neurological symptoms were observed in mice (ataxia, lethargy, seizures, weight loss or paralysis), the mice were sacrificed and tumor formation confirmed by tissue analysis using haematoxylin and eosin staining ⁸⁵. Single cells analysis of the tumor mass was achieved using flow cytometry to confirm DNA content as described in above. Briefly, cells were dissociated using Acutase to obtain a single suspension, viability was assessed using live dead near infrared stain, the cells were fixed in 4% paraformaldehyde, followed by fixation in methanol before staining using a PE-conjugated antibody specific for the neural cell surface marker (CD56) as described in ⁸⁵. Ploidy was assessed in viable, human tumor cells (as identified using human anti-CD56 antibody as described in ⁸⁵) positive cell subpopulations.

Statistical Analysis

The response between hyperdiploid cells and parent cultures to drug challenges, were reported for each treatment group as the standard error of the mean and represents data from 3 independent experiments unless stated otherwise. Data were input, graphed and analyzed using the software GraphPad Prism 5.0d for Mac. For comparing two samples, a two-tailed unpaired t-test was used to determine statistical significance. To compare three or more samples, two-way ANOVA with a Tukey post-test were used to determine statistical significance. In both cases p-values ≤ 0.05 were considered to be significant. *Denotes significance; **** $p \leq 0.0001$, *** $p \leq 0.001$ ** $p \leq 0.01$, * $p \leq 0.05$. Survival analysis for

xenotransplantation assays were performed using survival analysis function in Prism, survival proportions were plotted with data expressed as percent survival, the survival curves between hyperdiploidy and parent injected animals were compared using the Log-rank (Mantel-Cox) Test.

L-Lactate Metabolic Assays

GB cells grown under tumorsphere culture conditions were made into a single cell suspension and seeded at a density of 1×10^6 cells per ml and incubated for 24 hours under tumorsphere culture conditions. After 24 hours, L-Lactate levels were measured using the L-Lactate Assay Kit 1 manufactured by Eton Bioscience Incorporated following the manufacturer's instructions.

Cell Volume Measurement

GB cells grown under tumorsphere culture conditions were made into single cell suspension, fixed in 4% PFA in PBS, permeabilized in 100% ice cold methanol and 1×10^6 cells stained for DNA content using propidium iodide (PI) at a final concentration of $1 \mu\text{M}$ in PBS RNase solution for 30 minutes at room temperature as described in (cite). Cell Coulter volume was measured using a Beckman Coulter Quanta SC Flow Cytometer, and cell volume was calculated by the instrument software using $10 \mu\text{M}$ latex bead size standards.

CGH Analysis

DNA was extracted from GB tumorsphere cultures exactly as recommended in the NimbleGen Arrays User's Guide: CGH Analysis v5.1, and aliquots of DNA were shipped to NimbleGen for CGH analysis. The CGH array intensities were extracted by the NimbleGen software following their standard procedure. Segmented data were used to identify Copy Number Variants (CNVs) between each clone and the parent cell line. A segment was identified as amplified when the difference between the corrected log ratio for the Clone and the corrected log ratio for the Parent was greater than 0.3, and as deleted when smaller than -0.3. Common variants found in the Database of Genomic Variants (<http://projects.tcag.ca/variation>) were then filtered out. Genes affected by the remaining CNVs were annotated according to the build hg18 (provided with the array data) as reported in the UCSC Genome browser (<http://genome.ucsc.edu>). Pathways over-represented by the list of common genes between the three clones were identified with GeneGO (<https://portal.genego.com/>), with a False Discovery Rate (FDR) threshold of 0.05. Genes involved in pathways of interest (e.g. Cell Cycle, Cellular Growth and Proliferation, Cancer) were identified using Categories in the Ingenuity Pathway Analysis (IPA) software (<http://www.ingenuity.com/products/ipa>).

Results

1. Viable hyperdiploid GB tumor cells are present *in vitro* within tumorsphere cultures; and *in vivo* within xenograft and primary patient tumors.

Tumor cells isolated from primary patient GB tumors and maintained using serum free neurosphere culture conditions⁸⁸, a culture method hereafter referred to as tumorsphere cultures, preserves the genotype and phenotype of the original tumor during culture⁸¹. During cell cycle analyses of tumorsphere cultures, we noted the presence of a viable subpopulation of single cells that displayed elevated levels of genomic-DNA relative to the bulk-tumor population (Figure 1A). The proportion of cells in the total Glioblastoma tumor cell population determined as being hyperdiploid (4n+), ranged between 2- 10% under normal growth conditions. To determine if the hyperdiploid cell subpopulation is maintained during tumor formation, tumorsphere cultures were injected into the striatum of immune compromised mice. This xenograft model generates tumors with the histo-pathological features of high-grade glioma, and is an established experimental model for studying GB tumor initiation and disease progression^(85 and references therein). We injected 100,000 tumorsphere-derived GB tumorsphere cells into mice striatums, and analyzed the resulting tumors for the presence of viable hyperdiploid tumor cells. Consistent with our *in vitro* tumorsphere cell culture model, xenograft brain tumors derived from patient tumorsphere cell lines also contained a subpopulation of viable hyperdiploid cells (Figure 1B). To formally exclude the hypothesis that viable GB hyperdiploid cells are the product of our tumorsphere culture system, we examined primary patient tumor samples for evidence of viable hyperdiploid tumor subpopulations. In all patient samples examined, we could clearly identify a viable subpopulation of hyperdiploid cells present within the primary tumor specimen (Figure 1C), although the proportion of viable hyperdiploid cells varied between patients (Figure 1D).

Together, these results show a viable subpopulation of hyperdiploid tumor cells are present within patient GB tumors, and that this subpopulation is maintained during serum-free tumorsphere culture and in xenograft tumor models.

2. Clonal Hyperdiploid GB tumor cells can maintain long-term tumorsphere cultures and form tumors *in vivo* that have the histopathological features of high grade glioma.

Although hyperdiploid GB tumor cells are viable, model experimental systems have revealed that hyperdiploidy can generate a serious fitness cost for cells⁸⁹⁻⁹². Therefore hyperdiploidy may represent a cellular lineage that is an evolutionary dead-end within the GB tumor ecosystem. To begin to assess

the fitness cost of hyperdiploidy, we first attempted to isolate hyperdiploid clones from three primary patient GB tumorsphere cell lines. Multiple clonal cultures were isolated from all three lines that displayed hyperdiploid DNA content, which were tetraploid or near-tetraploid relative to the parental culture, were successfully isolated and expanded in culture (not shown). Three independent clonal hyperdiploid cultures derived from each patient line were assessed for their ability to proliferate and maintain long-term growth under tumorsphere culture conditions. All hyperdiploid clones could maintain long-term proliferation in serum-free culture conditions, although in most cases the proliferative rate for all clones was slightly less than the parental culture (Figure 2A). These results confirm that hyperdiploid clones are not only viable, but also possess the extensive proliferative capacity required to maintain long-term growth that is one of the hallmarks of cancer⁹³. We also estimated the ploidy of the hyperdiploid clonal cultures at passage 1 and passage 10 using flow cytometry. Hyperdiploid clones derived from Patient Line One displayed a relatively constant karyotype, maintaining an approximately two-fold DNA content throughout long-term culturing (Figure 2B). In contrast, hyperdiploid clones derived from Patient Lines Two and Three displayed evidence of genetic drift, with all of the hyperdiploid clonal lines losing DNA content during long-term culturing (Figure 2B). Altogether, these data suggest that in some patient lines hyperdiploidy is a relatively stable cell state that is maintained during growth, whereas in other patient lines hyperdiploid cells undergo genetic drift during repeated rounds of cell division.

Next, we directly assessed the ability of one of the hyperdiploid clones to form tumors using the xenograft intracranial tumor model⁸⁵. In all three patient lines both the parental and the hyperdiploid clones formed tumors *in vivo* (Figure 3A) that displayed histo-pathological features of high-grade gliomas (Supplementary Figure 3). Finally, we assessed the ploidy of the parent and hyperdiploid tumors by flow-cytometry. Parent injected tumours maintained a near-diploid DNA content and maintained a similar proportion of hyperdiploidy DNA content relative to the tumorsphere cultures (Figure 3B and data not shown). Intriguingly, the ability of clones to maintain a hyperdiploid state varied from patient to patient. The clonal line derived from Patient One maintained a relatively stable hyperdiploid state *in vivo* (Figure 3B upper panel). In contrast the clonal culture derived from Patient Two developed two distinct sub-populations *in vivo*, one of which displayed a sub-diploid karyotype (Figure 3B middle panel). Hyperdiploidy was lost *in vivo* from the clone derived from Patient Three, with the tumor displaying a subdiploid content as assessed by flow-cytometry.

These data sets show that GB hyperdiploid tumor cells are replication competent, maintain long-term proliferation in culture, and are able to form tumors. Moreover, we have shown that although in one

patient line hyperdiploidy can be stably maintained during long-term proliferation both in vitro and in vivo, in other patient lines the hyperdiploid is less stable and has the capacity to generate new karyotypes within the complex in vivo tumor micro-environment. Taken together, these data support the hypothesis that GB hyperdiploid cells represent a tumor subpopulation that has the capacity to positively contribute to GB disease progression and evolution.

3. Hyperdiploid GB tumor cells are resistant to conventional therapy.

As hyperdiploidy is an established mechanism for adaptation and therapy resistance in yeast⁹⁴⁻⁹⁶, and hyperdiploidy endows cancer cells with resistance to DNA damaging agents⁶⁸, we speculated that hyperdiploidy may provide survival advantages during conventional therapy in GB patients. To test this hypothesis we compared the response to therapy of the clonal hyperdiploid cultures to their parental culture, focusing on the more stable hyperdiploid clonal cultures derived from Patient One. These cell lines were tested routinely and maintained a stable hyperdiploid DNA content throughout this study (not shown). Hyperdiploid clonal cultures displayed elevated resistance to both therapies using TMZ and gamma radiation compared to their parental culture (Figure 4). Hyperdiploid cultures incubated with TMZ over 5 days are significantly more resistant to TMZ than their parental cultures (Figure 4A) with the hyperdiploidy clonal cultures significantly more viable than their parental cultures as determined using the MTT assay. Both parental and hyperdiploid cultures were exposed to 10 Gy doses of gamma radiation with hyperdiploidy clonal cultures displaying significantly more viability after radiation than the parental culture (Figure 4B), indicating that hyperdiploidy cells are more resistant to gamma radiation.

These observations support the hypothesis that the hyperdiploid cells are resistance against cytotoxic therapy, identifying GB hyperdiploid tumor cells as a tumor subpopulation of potential clinical relevance during disease recurrence after conventional therapy.

4. Hyperdiploid tumor cells cycle infrequently and are enriched within the label-retaining subpopulation.

Experimental data from yeast^{89, 90}, mammalian cell culture⁹¹ and tissue⁹² all indicate that hyperdiploidy reduces cellular proliferation. Consistent with a reduced proliferative phenotype, we have shown that GB hyperdiploid cells represent a subpopulation in primary tumor culture, mouse xenograft tumors and primary patient tumors. To formally address the replicative phenotype of GB hyperdiploid tumor cells, we analyzed the cell cycle distribution of the parent and tetraploid cells in

grown under tumorsphere culture conditions. Consistent with a reduced frequency of entering the cell cycle, the hyperdiploidy clonal tumorsphere cultures had a significant reduction in cells in G₂/M with a commensurate increase in the G₀/G₁ peaks (Figure 5A and 5B).

We then used two independent proliferation markers, Ki67 and phosphorylated retinoblastoma protein (phospho-RB), to assess the relative proliferation of the parent and hyperdiploid cultures. The Ki67 protein is expressed highly in proliferating cells, whereas exit from the cell cycle causes rapid loss of expression and protein degradation⁹⁷. The tight correlation between proliferation and Ki67 expression has made Ki67 expression a widely used marker to quantify the proportion of proliferating cells in the diagnosis and prognosis of many forms of cancer⁹⁸⁻¹⁰¹, including cancers of the brain^{102, 103}. The active, hypo-phosphorylated forms of Retinoblastoma protein (Rb) and the related Rb family members p107 and p130 block entry into S phase through inhibition of the E2F transcriptional program¹⁰⁴. Cyclin D- and cyclin E-dependent kinases phosphorylate the Rb proteins, which releases the Rb mediated block into S phase and allows cell division to proceed¹⁰⁴. Comparing tetraploid clones with their matched parental controls revealed that the tetraploid clones had on average 2.97% more *non-cycling* cells (as defined as negative for both phospho-RB and Ki67, p value = 0.0008) than the parental control (Figure 5C). Together with the DNA cell cycle analyses, these data indicate that hyperdiploid tumor cells cycle less frequently than euploid tumor cells, in part due to a delay during G₀/G₁ phase of the cell cycle.

To provide a functional readout of cell proliferation, we labeled the parental tumor-sphere culture with the pro-drug CFSE, which is converted by cellular esterases into a fluorescent compound covalently attached to proteins and retained within cells¹⁰⁵. CFSE is divided equally between daughter cells, allowing the quantification of cell proliferation¹⁰⁶. Infrequently cycling tumor cells that retain the dye (and hence are referred to as dye-retaining or label-retaining cells) have been identified in multiple tumor types¹⁰⁷⁻¹¹¹, including Glioblastoma⁸⁵. We labeled the tumor-sphere line with CFSE exactly as described in⁸⁵, and seven days later analyzed the DNA content of the bulk population and the label retaining cells. Strikingly, the prevalence of hyperdiploidy was inversely proportional to proliferation, with label retaining cells displaying a marked elevation in hyperdiploid cells (Figure 5D). We repeated this experiment using the other two patient tumor lines (Patient Line 2 and Patient Line 3), and found that in all three patient tumorsphere lines, with the frequency of hyperdiploid cells increased within the infrequently cycling, label-retaining cell subpopulation in all three patient lines (Supplementary Figure 4).

The cell cycle analyses showing hyperdiploid tumor cells have an increased G_0/G_1 and reduced G_2/M DNA content, a reduced number of cells expressing proliferation markers, and an enrichment of hyperdiploid cells within the label retaining population, all support the hypothesis that hyperdiploid tumor cells cycle less frequently than their euploid counterparts.

5. Hyperdiploid tumor cells display unique hyperdiploid karyotypes relative to the parental euploid population.

Direct comparison of genomic content by flow cytometry shows that the hyperdiploidy clones revealed that the isolated clones had close to double the genomic content than the parent euploid population (Figure 6A). To determine whether hyperdiploidy clones are the result of simple chromosomal doubling (i.e. tetraploidy), or express unique karyotypes with specific chromosomal gains and/or losses, we performed CGH analyses on the parent and hyperdiploidy clone populations derived from Patient One. Examination of the CGH data at low resolution showed chromosomal gains and losses unique to the hyperdiploid clones (Figure 6B and Supplementary Figure 5). From the segmented CGH Array data, we identified 284 genomic regions across 16 chromosomes with an average log ratio greater than 0.3 or smaller than -0.3, corresponding to a gain or loss respectively between any clone and the parent (Supplementary Table 1). The high resolution afforded by the CGH analyses revealed two important points. First, hyperdiploid clones display chromosomal gains and losses compared to the euploid parent population, revealing that clones are not true tetraploid cells, but are hyper-diploid with near-tetraploid chromosomal content (Figure 6 and Supplementary Table 1). We identified the genes affected by copy number variations using their chromosomal positions from the UCSC hg18 build: 1297 genes were found as overlapping CNV regions (in any proportion) in any clone (Supplementary Table 2), of which only 16 genes were in common between the three clones (Table 1). Thus the second important conclusion is that each hyperdiploid clone is made up of a karyotype containing a unique combination of amplifications and deletions.

Despite the finding that there was little overlap between genes amplified or deleted between the three clones, it is possible that conserved biological functions were modified in all three clones by targeting different parts of the same networks. As a first-pass assessment of this hypothesis, we uploaded the list of affected genes in any of the three clones into the MetaCore™ pathway analysis tool (GeneGo) in order to identify over-represented pathways. Pathways identified with a p-value smaller than 0.05 were reported. Of particular interest, pathways related to translation regulation, apoptosis and survival, and cell cycle are found with the highest significance (Table 1). The Ingenuity Pathway Analysis (IPA)

software was also used to investigate at a higher level the functional networks over-represented in the list of affected genes common to the three clones. So called “IPA Categories” identified with a p-value smaller than 0.05 include “Cellular Growth and Proliferation”, “Cancer”, “Cell Cycle”, “Cell Death and Survival” and “DNA Replication, Recombination, and Repair” (Table 1). Recently, Amon and Colleagues characterized a series of mutations that compensate for the fitness cost associated with aneuploidy¹¹². We therefore interrogated our CGH data sets for gene amplifications that corresponded to aneuploidy-tolerating mutations found in yeast. Intriguingly, we identified several genes amplified within GB hyperdiploid clones that corresponded to aneuploidy-tolerating mutations identified in yeast (Table 2).

The small percentage of common genes that amplified or deleted in all three hyperdiploid clones suggests that the hyperdiploid tumor cell subpopulation is made up of genetically heterogeneous cells expressing a variety of hyper-diploid karyotypes. It is possible that there exists a range of hyperdiploidy-tolerating mutations that modify core cellular processes that compensate for the deleterious effects of hyperdiploidy and contribute the maintenance of a viable, hyperdiploid subpopulation within patient tumors. Our initial pathway analyses indicating that changes in gene expression within the ubiquitin proteome system occur in all three hyperdiploid clones provide preliminary support for this hypothesis.

6. Hyperdiploid tumor cells are larger, more metabolically active, and more sensitive to 2-DG than parental euploid cells.

Cell size scales linearly with DNA content in Eukaryotes¹¹³⁻¹¹⁶, and cell size is proportional to ploidy status, with diploid yeast cells being approximately twice the size of haploids^{117, 118}. Based on these historical data sets, we predicted that large cell size is a phenotype that is conserved throughout the hyperdiploid tumor cell population, which could be used as a foundation for developing specific anti-hyperdiploid therapeutic strategies.

To determine whether GB hyperdiploidy cells are proportionally larger than the euploid bulk population, we first compared the volume of tetraploid clones to their parental euploid controls. Consistent with historic studies¹¹³⁻¹¹⁸, GB hyperdiploid tumor cells are approximately twice as large as their euploid counterparts. This increase is proportional to the roughly twofold increase in the genomic content of the hyperdiploid tumor cells (Figure 7A). One potential consequence of large cell size is increased metabolic demand, as bigger cells are likely to require more energy to grow to a sufficient cell volume to allow for cell doubling^{119, 120}. We therefore measured glycolysis, a primary metabolic

pathway in tumor cells¹²¹. Specifically, we assessed the production of L-Lactate, an established marker for glycolysis in tumor cells¹²². Consistent with increased cell size, hyperdiploid tumor cells displayed a higher metabolic rate than the euploid control population (Figure 7B). The large cell size and increased metabolism of hyperdiploid tumor cells may represent a point of fragility specific to the hyperdiploid subpopulation that could be exploited therapeutically. To test this hypothesis, we treated parental euploid and hyperdiploid clonal cultures with the 2-deoxy-D-glucose (2-DG), an established inhibitor of glycolysis¹²³⁻¹²⁶. Strikingly, we found that the hyperdiploid clones were significantly more sensitive to the effects of glycolysis inhibition than the euploid parent control (Figure 7C).

Together, these results support the hypothesis that hyperdiploid tumor cells are large and have a commensurately higher metabolic requirement than euploid tumor cells. These findings suggest that inhibiting tumor metabolism may be an effective therapeutic strategy to specifically target hyperdiploid tumor cells, a hypothesis supported by the observation that hyperdiploidy clonal populations are more sensitive to the effects of glycolysis inhibition compared to the euploid parent tumor cell control.

Discussion

It is now clear that phenotypic heterogeneity in solid tumors is a major player determining patient response to therapy and the evolution of therapy resistance². The challenge for researchers is to begin the design and development of therapeutic strategies that reduce tumor heterogeneity in an effort to extend the efficacy of hard-won frontline therapies². As therapy resistance is driven, at least in part, through the selection of resistant clones from a heterogeneous tumor cell population, a potential strategy to delay the emergence of therapy resistance in patients during treatment is to deplete therapy resistant clones before and/or during therapy. The identification and characterization of therapy resistant cells from tumor cell populations is the crucial first step towards this goal. Here we have identified a hyperdiploid tumor cell subpopulation of potential clinical significance that is present in adult brain GB tumors. These cells are viable, able to maintain long-term proliferation and drive tumor growth *in vivo*, and are resistant to conventional therapy.

Despite the observation that almost all cancers cells have degrees of aneuploidy¹²⁷, the contribution of genetic imbalance to the pathophysiology of cancer remains an ongoing question in cancer research. Direct experimental evidence supporting a pivotal role for polyploidy in tumor initiation has been provided in a series of seminal studies¹²⁸⁻¹³¹, however the role of hyperdiploidy in advanced disease is less well understood. It was first hypothesized by Boveri¹³² that aneuploidy may cause the uncontrolled proliferation of cancer cells. This hypothesis has been countered with experimental

observations showing that aneuploidy, in particular polyploidy, reduces cellular proliferation. For example studies of aneuploidy yeast strains have widely characterized that aneuploidy strains have a proliferative disadvantage^{89, 90}. The growth disadvantage of aneuploidy has also been demonstrated in mammalian cells derived from aneuploid mice, where aneuploid cells showed proliferation defects under standard tissue culture conditions⁹¹. In tissues, polyploidy is associated with a markedly decreased replicative capacity (reviewed in⁹²). Consistent with the idea of hyperdiploidy providing a growth disadvantage in adult brain cancer, GB hyperdiploid clonal cultures were less proliferative than the parental tumor cell population. Cell cycle analyses confirmed that hyperdiploid tumor cells cycle less frequently than the euploid tumor bulk, which is caused (at least in part) by a delay in G₀/G₁. Altogether, our data and historic studies all support the hypothesis that hyperdiploidy comes with the fitness cost of decreased replicative capacity.

The reduced proliferative capacity of hyperdiploid tumor cells would be predicted to provide a selective disadvantage in the competitive tumor environment; a prediction borne out by the observation that hyperdiploid cells represent a relatively small cell subpopulation within patient and xenograft tumors as well as during growth under tumorsphere cell culture conditions. However, this situation can change during the therapeutic selection pressures that occur during treatment. We have shown here that GB hyperdiploid cells are resistant to DNA damaging therapies gamma radiation and temozolomide. These results are consistent with tetraploid models of colon carcinoma, in which tetraploidy (a specific form of hyperdiploidy) was shown to provide resistance to DNA-damaging agents⁶⁸.

Infrequent cell cycle is a well-established drug resistance mechanism, and provides a plausible explanation as to why GB hyperdiploid tumor cells are resistant to DNA gamma radiation and temozolomide. Quiescent (G₀) haematopoietic stem cells (HSCs) are resistant to the anti-proliferative chemo-therapeutic agent 5-fluoro-uracil (5-FU)^{133, 134}, and become sensitive to 5-FU treatment when they are forced from G₀ into a proliferative state by treatment with IFN α ¹³⁵. Further, HSCs can be protected from the effects of irradiation by increasing the proportion of HSCs in G₀ through a variety of treatments in vivo¹³⁶⁻¹³⁸. In cancer, the chemo-protective effect of cell cycle-mediated drug resistance is well established¹³⁹. For example, Schmidt and colleagues demonstrated that colon adenocarcinoma cells arrested in G₁ by over-expression of p27^{Kip1} are significantly more resistant to a variety of chemo-therapeutic agents, including temozolomide¹⁴⁰. Using a mouse xenograft model, Naumov et al showed that the DNA intercalating compound doxorubicin (DXR) effectively reduced the metastatic tumor burden but spared non-cycling tumor cells, which persisted during therapy and subsequently developed into metastases after DXR therapy was discontinued¹⁴¹. More recently, label-retention has been used to

phenotypically identify infrequently dividing cells that are resistant to chemotherapy from a variety of tumor types^{109, 142-144}. Studies examining the cancer stem cell phenotype have also shown that quiescence provides protection against cell death induced by DNA-damage agents^{145, 146} and chemotherapy¹⁴⁷. Recently, a landmark study by Kreso et al revealed how chemotherapy selects for minor, infrequently cycling subpopulations using lineage tracking in mouse models of cancer evolution¹⁴⁸. Collectively these studies provide strong support the hypothesis that infrequent cell cycle contributes to the evolution of therapy resistance in cancer, and here we identify hyperdiploidy as an additional mechanism to generate slow-cycling cell subpopulations within solid tumors.

Why do hyperdiploid tumor cells cycle less frequently? One intriguing possibility is that the difference in cell size between hyperdiploid and diploid cells determines the frequency of cell division. We found that GB hyperdiploid tumor cells have a two-fold larger cell volume compared to their diploid counterparts. Cell growth, cell size and cell division are co-regulated to ensure cells are large enough to divide at mitosis¹⁴⁹. Studies in yeast revealed a size requirement for G₁-S transition, with smaller cells delaying in G₁ until a sufficient size was reached to maintain viable progeny after cell division^{150, 151}. Complementary studies in animal cells show that mammalian cells also delay in G₁ to allow an appropriate cell size to be achieved^{119, 120}. Thus one plausible hypothesis is that the larger hyperdiploid tumor cells arrest during G₀/G₁ to allow for a sufficient growth to occur before committing to division.

Hyperdiploidy may contribute to therapy resistance through additional mechanisms other than cell cycle effects. Both temozolomide and ionizing radiation inhibit the proliferative capacity of tumor cells by inducing senescence¹⁵²⁻¹⁵⁴. A recent study has shown that hyperdiploid cells preferentially escape from therapy induced senescence, providing another mechanism for hyperdiploid tumor cells to resist the effects of conventional therapy⁶⁹. Hyperdiploidy also generates phenotypic changes through changes in gene expression^{95, 155}, and there is a growing body of evidence suggesting that hyperdiploidy-dependent phenotypic changes provide adaptive advantages during therapy in a wide range of clinical settings. In fungal pathogens, chromosomal gains are thought to be responsible for anti-fungal drug resistance and immune-evasion (reviewed in^{156, 157}). In experimental yeast models of therapy resistance, chromosomal gains provide a selective advantage under chemotherapeutic, cytotoxic and anti-fungal drugs^{95, 96}. Bortezomib (Velcade) is an important drug for the treatment of multiple myeloma (MM). In a myeloma cell line model of cancer therapy resistance, hyperdiploid myeloma cells display a five-fold resistance to the proteasome inhibitor bortezomib (Velcade) that is associated with over-expression of the proteasome subunit PSMβ5, the cellular target of bortezomib⁷⁰. Our CGH analyses show that hyperdiploid clones contain unique chromosomal gains and losses, and

these could also contribute to the evolution of therapy resistance through the generation of novel therapy-resistant phenotypes. It is also possible that hyperdiploid cells are more resistant to genomic toxins due to simple gene duplication, which could preserve gene function through redundancy mediated genetic buffering¹⁵⁸. It must also be noted that genotoxins such as TMZ and γ -radiation directly cause the generation of hyperdiploidy within GB patients, based on the classic study by Yung and colleagues³² and more recent results obtained in breast cancer⁷¹. Lagadec and colleagues increased the prevalence of hyperdiploidy using radiation or pharmacological induction and showed that the resulting hyperdiploid tumor cells display a pluripotent, tumor-initiating phenotype⁷¹. These data support the provocative hypothesis that radiotherapy increases the aggressiveness of a patient tumor by elevating the frequency of hyperdiploid cells within the surviving tumor cell population⁷¹. Altogether there is a growing body of literature that provides a strong precedent for the ability of hyperdiploid cells to contribute to the evolution of therapy resistance and disease recurrence in advanced disease. Our study suggests that this hypothesis also holds true for adult brain cancer.

The causes and consequences of aneuploidy is currently an area of intense research (reviewed in¹⁵⁹⁻¹⁶¹). Our CGH analyses of hyperdiploid clones revealed that each clone displayed a unique karyotype, suggesting that the GB hyperdiploid subpopulation is composed of cells that are genetically heterogeneous, expressing a variety of complex karyotypes. Although we identified 16 common genes amongst the three clones that showed either gains or losses that were specific to the polyploidy cell lines analyzed, a systematic analysis of a large cohort of primary hyperdiploid tumor samples, in combination with specific cell biology experiments in established experimental models of aneuploidy, will be required to formally determine the role of these genes in generating and/or maintaining a hyperdiploid phenotype. Our finding that different hyperdiploid cells display various levels of chromosomal stability reveals further complexity that is inherent to the hyperdiploid phenotype. Shackney et al proposed that aneuploidy cancers develop from an unstable tetraploid precursor¹⁶², and there is now strong evidence from multiple tumor types that aneuploidy can indeed develop from a transient tetraploid state (reviewed in¹⁵⁹). In two of the patient lines studied here, hyperdiploid lines displayed an unstable phenotype during long-term culture in vitro, and both lines generated near-diploid progeny within xenograft tumors. These data suggest that in adult brain cancer, genetically unstable hyperdiploid tumor cells may function as a transient gateway cell state that enables the generation of novel genotypes, thereby facilitating rapid tumor evolution during advanced stages of the disease.

Several independent groups have made inroads into the development of therapeutic strategies that target aneuploidy¹⁶³, and more specifically hyperdiploid tumor cells⁷³⁻⁷⁷. We have shown that hyperdiploid tumor cells have a two-fold increase in cell volume that is proportional to their approximately doubled genome. As the positive relationship between genome size and cell volume has been evolutionarily conserved throughout eukaryotes¹¹³⁻¹¹⁶, a larger cell volume may be a common phenotype within the hyperdiploid tumor cell subpopulations, which may increase the sensitivity of hyperdiploid tumor cells to inhibitors of tumor metabolism. Consistent with this hypothesis, hyperdiploid clonal cultures were more metabolically active than the diploid lines, and showed an increased sensitivity to inhibition of glycolysis. Further, seminal studies in yeast have revealed aneuploid yeast cells with extra chromosomes require more glucose for survival than wild-type cells⁸⁹. Together these results suggest that tumor metabolism may be a point of fragility within hyperdiploid tumor cells that can be therapeutically exploited to target this subpopulation within patient tumors. Our hope is that this insight will contribute to the development of anti-hyperdiploid treatments, which can be used to reduce cellular heterogeneity in solid tumors and maintain the efficacy of frontline therapies.

Acknowledgements

This work is an initiative of the Queensland Neurosurgery Research Fund (QNRF)

This work was supported by funding from the Brain Foundation, the Australian National Health and Medical Research Council (NHMRC) Grant Number APP569662, and the Australian Research Council (ARC) Grant Number DP1094181

Figure Legends

Figure 1. Human Glioblastoma cells harbor a population of hyperdiploidy cells that are maintained in tumorsphere cultures and in xenograft mouse tumors.

(A) The DNA content of single, viable, tumorsphere cells was compared to a CFSE labeled diploid control to determine the frequency of hyperdiploid cells in tumorsphere cultures. Compared to CFSE labeled diploid NFF control cultures, the bulk of the parent population has a sub-diploid DNA content. However, a viable subpopulation of cells with elevated DNA content ($4n+$) was observed in all tumorsphere cultures. Using this method it was determined that hyperdiploid cells represent 5.88% ($\pm 1.075SD$, $N=3$) of the bulk tumorsphere population.

(B) Primary human Glioblastoma tumor cells maintained under tumorsphere culture conditions were injected into the striatum of five immune-compromised mice per line (five mice injected with control, five mice injected with hyperdiploid clonal culture to derive survival curves) and tumors were allowed to form *in vivo*. Three of resulting tumors for each condition were harvested, dissociated into single cells and viable cells were identified by flow cytometry and analyzed for DNA content. As in the tumorsphere cultures, a subpopulation of hyperdiploid cells representing 7.88 % ($\pm 0.3878SD$, $N=3$) was identified, indicating that hyperdiploid cells are capable of forming tumors and are maintained during tumorigenesis.

(C) Viable hyperdiploid Glioblastoma cells were identified in single cell suspensions of patient tumor biopsy samples using multiplex flow-cytometry protocol. The DNA content of single, viable tumor cells were analyzed to determine the frequency of hyperdiploid cells in primary tumors. Cell cycle analyses identify a subpopulation of viable primary tumor cells with elevated DNA content in all tumors assessed. Using this method the mean frequency of hyperdiploid cells in human Glioblastoma was determined to be 4.89% ($\pm 3.704SD$, $N=6$) of the bulk tumor population.

(D) A box and whisker plot showing the distribution of hyperdiploid cells in single cell suspension from human Glioblastoma tumors, tumorsphere cultures and xenograft mouse tumors, there is not a significant difference in the mean number of hyperdiploid cells between the three conditions as determined by one way-ANOVA.

Figure 2. Hyperdiploid tumor cells maintain long-term cultures and display a pseudo-stable karyotype in vitro.

(A) Three clonal cultures were derived from three independent primary patient tumorsphere lines and identified as hyperdiploid by flow-cytometry (not shown), were amplified as tumor spheres in identical conditions as their parent bulk population, and then propagated under long term passaging. All three parents (shown in red) and their three respective clones (shown in blue) were viable (as determined by trypan blue exclusion assay) and maintained growth over 10 passages (corresponding to an 11 week culturing period). For the clonal cultures derived from Line 1, the number of cells generated over long-term culturing period was significantly less than the parental cultures. On average over 10 passages, the parental culture would generate 17.6 ± 1.2 (N=10) times more cells than were initially seeded. The growth factor of clones was significantly less, with Clone 1 growing at a rate of 7.269 ± 1.203 (N=10, $p \leq 0.0001$), Clone 2 at 9.693 ± 1.169 (N=10, $p \leq 0.0001$) and Clone 3 at 4.159 ± 1.386 (N=10, $p \leq 0.0001$).

(B) The relative ploidy of the hyperdiploid clones at passage one and passage ten was determined by flow-cytometry by comparing DNA content of the $2n$ peak of the tumor line to the diploid control line as outlined in the Material and Methods. Hyperdiploid clones derived from Patient One primary tumorsphere line displayed a relatively stable karyotype and maintained an approximate two-fold DNA content over ten passages. In contrast, the hyperdiploid clones generated from the tumorsphere lines of Patients Two and Three showed a loss of DNA content at passage ten compared to the original culture at passage one. The parent controls for each line did not display any significant change in DNA content (not shown), with the final passage of the parent controls shown as a reference.

Figure 3. Hyperdiploid tumor cells can initiate tumor formation and display various levels of genomic stability in vivo.

(A) Kaplan-Meier survival curve of tumor-progression in mice injected with three parental and a single hyperdiploid clonal cultures. Single cells derived from either the parental or a hyperdiploid clone tumorsphere culture were injected into the striatum of five SCID mice (1×10^6 cells/mouse) and allowed to form tumors. Shown are the Kaplan-Meier survival curves comparing the progression of five control mice (parental cell population) versus five mice injected with the hyperdiploid tumor cells, with all mice forming tumors.

(B) Stability of polyploid cells in xenografts. The CD45⁻/CD56⁺, viable cell population in xenograft tumors was identified and then the DNA content of the 2n tumor cell peak normalized to the 2n content diploid control 2n content as outlined in the Material and Methods. The clone derived from Patient Line 1 (upper panel) displayed some genetic drift, but nevertheless maintained an approximate two-fold DNA content in vivo. In contrast, the tumor generated from the hyperdiploid clone derived from Patient Line 2 (middle panel) developed two distinct subpopulations as determined by flow cytometry, one of which displayed a marked loss of DNA content and a separate population that maintained two-fold DNA content. The tumor generated from the hyperdiploid clone of Patient Line Three (lower panel) showed a marked loss of DNA content in vivo.

Figure 4. Hyperdiploid cells are resistant to conventional therapy.

(A) MTT assay measuring cell viability in cells treated with temozolomide. Parental tumorsphere cultures (N= 3) and hyperdiploid clonal cultures (N = 3 for each clone) were treated with 60 μ M temozolomide and viability measured 7 days after treatment. All three hyperdiploid clonal populations were significantly more resistant to temozolomide than the parental control population.

(B) MTT assay measuring cell viability in cells treated with γ -radiation. Parental tumorsphere cultures and hyperdiploid clones were treated with a single dose of gamma radiation (10 Gy), changes in viability after 7 days in culture was monitored using the MTT assay. Parent tumorsphere cultures were sensitive to killing by gamma radiation, 9.2% (\pm 1.2%,N=8) of cells remained viable in the culture period. By comparison, all hyperdiploid clones were resistant to radiation induced cell death with 19.9%(\pm 2.4%,N=8) of cells remaining viable in hyperdiploid clone 1, 23.6% (\pm 4.4%,N=8) of cells remaining viable in hyperdiploid clone 2 and similar resistance was observed in hyperdiploid clone 3 (26.9 \pm 1.9%, N=8).

*Denotes significance as determined by ANOVA with Tukey post-test; **** p \leq 0.0001, *** p \leq 0.001 ** p \leq 0.01, * p \leq 0.05.

Figure 5. Hyperdiploid cells cycle less frequently than euploid tumor cells.

(A) Typical DNA histograms of Parent Euploid and Hyperdiploid clonal cultures. Relative to the Parent control, Hyperdiploid clones have a reduced number of cells in the G₂/M phases of the cell cycle.

(B) Statistical analysis of the cell cycle using data derived from three independent Parent and Clonal cultures grown as tumorspheres. Compared to the Parent control, hyperdiploid clones display an increase in G_0/G_1 and a loss of G_2/M , consistent with a delay in the G_0/G_1 phase of the cell cycle. Significance was determined using ANOVA using TUKEY post-test, *** $p \leq 0.001$.

(C) Comparison of two proliferation markers between parent euploid and hyperdiploid clonal cultures. Parent and Polyploid Clones were grown under tumorsphere culture conditions for 5 days, then harvested as single-cell suspension. The Parental population was bar-coded using CFSE, and then all cell populations were fixed and permeabilized for flow-cytometry. After blocking, each clone was mixed with bar-coded parent control and the mixed populations stained for phosphorylated RB (phospho-Rb, y axis) and Ki67 (x axis). Each clone displayed a reduced number of double-positive proliferating cells (phospho-Rb/Ki67 positive, top right quadrant) and an elevated number of non-cycling, double negative cells (phospho-Rb/Ki67 double negative, bottom left quadrant) relative to the matched Parental control population exposed to identical staining conditions within the same tube.

(D) Hyperdiploid tumor cells are enriched within the slow-cycling, label retaining subpopulation. The Parental population was stained with CFSE and then cultured for 7 days under tumorsphere culture conditions. CFSE is diluted with each cell division; after 7 days infrequently dividing cells can be identified as the label-retaining, CFSE-high subpopulation of cells. The left panel shows the distribution of CFSE after 7 days and two gates that identify the top 25% and top 5% CFSE-High cells. Analysis of the DNA content of the bulk population shows a typical cell-cycle distribution between the 2n and 4n peaks. Analyzing the DNA content of the Top 25% and Top 5% CFSE subpopulations revealed that the 4n and 8n peaks increased with label-retention, showing that the proportion of hyperdiploid cells increased within the label-retaining, infrequently cycling cells. The percentage of cells within the 8n gate, from both the total population and the label-retaining population, were determined from four independent experiments. The total population had on average 2.9% of cells within the 8n gate, whereas the label retaining had 17.4% 8n cells (p value = 0.0059).

Figure 6. Hyperdiploid tumor cells display a complex hyperdiploid karyotype relative to the tumor bulk.

(A) Parent and hyperdiploid clonal cultures grown under neurosphere conditions were harvested as single cells, the parent control population stained with CFSE, then fixed and permeabilized for flow cytometry. Each clonal population was spiked with a CFSE-labelled parent control population and the mixture stained for DNA content using DAPI. During analysis the parent control and clone were

identified based on CFSE staining intensity (left panel) and histograms overlaid to allow comparison of the DNA content of the clones relative to the parent control.

(B) CGH data summarized in visual format were used to detect obvious chromosomal gains and/or losses present within the hyperdiploid clone compared to the parental control. All three clones displayed both gains and losses relative to the parental bulk population.

Figure 7. Hyperdiploid tumor cells are larger, more metabolically active, and more sensitive to glycolysis inhibition than euploid tumor cells.

(A) Parent control and hyperdiploid clonal cultures grown under tumorsphere conditions were stained for DNA content and analyzed for cell volume using BD Quanta flow cytometer. The G₀/G₁ cell population was identified by DNA content (upper left panel), and the electronic volume for the parent and clone G₀/G₁ cells determined from 10,000 cells. The panels show the electronic volume distribution of the Parent (red curve) and the hyperdiploid Clones (blue curves). The mean cell volume for the Parent and Clones G₀/G₁ cells was calculated from 10,000 cells using 10 μm diameter beads to determine cell volumes.

(B) Parent and hyperdiploid Clone cultures were seeded in tumorsphere conditions at a density of 1x10⁶ cells/ml, and the amount of L-Lactate measured 24 hours later. Shown is the mean relative L-Lactate production measured from three independent cultures per sample. Significance was determined using ANOVA using TUKEY post-test, *** p ≤ 0.001.

(C) Parental tumorsphere cultures (N = 3) and hyperdiploid clonal cultures (N = 3 for each clone) were treated with 4 mM 2-Deoxy-D-glucose (2-DG) and viability measured 7 days after treatment. All three hyperdiploid clonal populations were significantly more sensitive to 2-DG than the parental control population. *Denotes significance as determined by ANOVA with Tukey post-test; **** p ≤ 0.0001, *** p ≤ 0.001.

Table 1. List of Copy Number Variations (CNVs) in hyperdiploid clones.

Using the segmented CGH Array data, we identified 284 genomic regions across 16 chromosomes with an average log ratio greater than 0.3 or smaller than -0.3, corresponding to a gain or loss respectively between any clone and the parent. The 16 genes described in this table were changed in all three clones.

Table 2. Aneuploidy tolerating mutations in yeast found to be amplified in hyperdiploid human Glioblastoma cells.

We interrogated our CGH data sets for gene amplifications that corresponded to aneuploidy-tolerating mutations found in yeast. In all three clones we identified genes that are associated with the ubiquitin proteasome system amplified within GB hyperdiploid clones, which corresponded to aneuploidy-tolerating mutations identified in yeast¹¹².

Gene Name	Clone 1 vs Parent		Clone 2 vs Parent		Clone 3 vs Parent		Protein Name
	GENE %	CNV ratio	GENE %	CNV ratio	GENE %	CNV ratio	
B3GNTL1	23%	-0.30	23%	-0.34	23%	-0.34	UDP-GlcNAc:betaGal beta-1,3-N-acetylglucosaminyltransferase-like 1
CLTC	88%	-0.32	88%	-0.32	88%	-0.33	CLTC clathrin, heavy chain (Hc)
DHX40	100%	-0.32	100%	-0.32	100%	-0.33	DHX40 DEAH (Asp-Glu-Ala-His) box polypeptide 40
EGFR	100%	-0.95	100%	-1.13	100%	-0.58	EGFR epidermal growth factor receptor
FLJ40504	100%	-0.31	100%	-0.35	100%	-0.34	KRT18P55 keratin 18 pseudogene 55
FOXJ1	100%	-0.30	100%	-0.37	100%	-0.35	FOXJ1 forkhead box J1
HPVC1	100%	-0.95	100%	-1.13	100%	-0.58	HPVC1 human papillomavirus (type 18) E5 central sequence-like 1
LRP1B	13%	-0.51	6%	0.56	6%	0.53	LRP1B low density lipoprotein receptor-related protein 1B
NLK	95%	-0.31	11%	-0.35	11%	-0.34	NLK nemo-like kinase
PPY2	100%	-0.31	100%	-0.35	100%	-0.34	PPY2 pancreatic polypeptide 2
PYY2	100%	-0.31	100%	-0.35	100%	-0.34	PYY2 peptide YY, 2 (pseudogene)
RNF157	100%	-0.30	100%	-0.37	100%	-0.35	RNF157 ring finger protein 157
SEC61G	100%	-0.95	100%	-1.13	100%	-0.58	SEC61G Sec61 gamma subunit
TBCD	54%	-0.30	54%	-0.34	54%	-0.34	TBCD tubulin folding cofactor D
VSTM2A	100%	-0.95	100%	-1.13	100%	-0.58	VSTM2A V-set and transmembrane domain containing 2A
ZNF750	11%	-0.30	11%	-0.34	11%	-0.34	ZNF750 zinc finger protein 750

Table 1 List of Copy Number Variations (CNVs) in hyperdiploid clones.

Gene Symbol	Name	Yeast ortholog	% Amplification in polyploid clones	GO Molecular Function	GO Pathway
Nedd4	Neuronally Expressed Developmentally Downregulated 4 Ubiquitin protein Ligase	Nedd4	66.6	Ubiquitin-protein ligase activity	Ubiquitin proteasome system
USP14	Ubiquitin carboxyl-terminal hydrolase 14	USP14	33.3	Ubiquitin-protein ligase activity	Ubiquitin proteasome system
PRS7	26S protease regulatory subunit 7	PSMC2	33.3	Hydrolase activity	Ubiquitin proteasome system
SAS10	Something about silencing protein 10	UTP3	33.3	RNA binding	Ubiquitin proteasome system

Table 2. Aneuploidy tolerating mutations in yeast found to be amplified in hyperdiploid human Glioblastoma cells.

References

1. P. C. Nowell, *Science*, 1976, 194, 23-28.
2. T. Tian, S. Olson, J. M. Whitacre and A. Harding, *Integr Biol (Camb)*, 2010, 3, 17-30.
3. M. Gerlinger and C. Swanton, *Br J Cancer*, 2010, 103, 1139-1143.
4. M. Greaves and C. C. Maley, *Nature*, 2012, 481, 306-313.
5. R. J. Gillies, D. Verduzco and R. A. Gatenby, *Nature Reviews. Cancer*, 2012, 12, 487-493.
6. A. Marusyk, V. Almendro and K. Polyak, *Nature Reviews. Cancer*, 2012, 12, 323-334.
7. T. A. Yap, M. Gerlinger, P. A. Futreal, L. Pusztai and C. Swanton, *Science Translational Medicine*, 2012, 4, 127ps110.
8. L. R. Yates and P. J. Campbell, *Nature Reviews. Genetics*, 2012, 13, 795-806.
9. S. Kobayashi, T. J. Boggon, T. Dayaram, P. A. Janne, O. Kocher, M. Meyerson, B. E. Johnson, M. J. Eck, D. G. Tenen and B. Halmos, *N Engl J Med*, 2005, 352, 786-792.
10. M. E. Gorre, M. Mohammed, K. Ellwood, N. Hsu, R. Paquette, P. N. Rao and C. L. Sawyers, *Science*, 2001, 293, 876-880.
11. N. P. Shah, J. M. Nicoll, B. Nagar, M. E. Gorre, R. L. Paquette, J. Kuriyan and C. L. Sawyers, *Cancer Cell*, 2002, 2, 117-125.
12. C. Roche-Lestienne and C. Preudhomme, *Semin Hematol*, 2003, 40, 80-82.
13. C. R. Miller and A. Perry, *Arch Pathol Lab Med*, 2007, 131, 397-406.
14. W. Stummer, U. Pichlmeier, T. Meinel, O. D. Wiestler, F. Zanella, H. J. Reulen and A. L.-G. S. Group, *The Lancet Oncology*, 2006, 7, 392-401.
15. W. Stummer and M. A. Kamp, *Current Opinion in Neurology*, 2009, 22, 645-649.
16. N. Laperriere, L. Zuraw, G. Cairncross and G. Cancer Care Ontario Practice Guidelines Initiative Neuro-Oncology Disease Site, *Radiotherapy and Oncology : Journal of the European Society for Therapeutic Radiology and Oncology*, 2002, 64, 259-273.
17. R. Stupp, W. P. Mason, M. J. van den Bent, M. Weller, B. Fisher, M. J. Taphoorn, K. Belanger, A. A. Brandes, C. Marosi, U. Bogdahn, J. Curschmann, R. C. Janzer, S. K. Ludwin, T. Gorlia, A. Allgeier, D. Lacombe, J. G. Cairncross, E. Eisenhauer and R. O. Mirimanoff, *N Engl J Med*, 2005, 352, 987-996.
18. M. Koshy, J. L. Villano, T. A. Dolecek, A. Howard, U. Mahmood, S. J. Chmura, R. R. Weichselbaum and B. J. McCarthy, *Journal of Neuro-oncology*, 2012, 107, 207-212.
19. K. Rock, O. McArdle, P. Forde, M. Dunne, D. Fitzpatrick, B. O'Neill and C. Faul, *The British Journal of Radiology*, 2012, 85, e729-733.
20. B. Tran and M. A. Rosenthal, *J Clin Neurosci*, 2010, 17, 417-421.
21. A. Giese, R. Bjerkvig, M. E. Berens and M. Westphal, *Journal of Clinical Oncology : Official Journal of the American Society of Clinical Oncology*, 2003, 21, 1624-1636.
22. S. Bao, Q. Wu, R. E. McLendon, Y. Hao, Q. Shi, A. B. Hjelmeland, M. W. Dewhirst, D. D. Bigner and J. N. Rich, *Nature*, 2006, 444, 756-760.
23. R. Bonavia, M. M. Inda, W. K. Cavenee and F. B. Furnari, *Cancer Res*, 2011, 71, 4055-4060.
24. J. R. Shapiro, W. K. Yung and W. R. Shapiro, *Cancer Res*, 1981, 41, 2349-2359.
25. C. J. Wikstrand, S. H. Bigner and D. D. Bigner, *Cancer Res*, 1983, 43, 3327-3334.
26. M. Snuderl, L. Fazlollahi, L. P. Le, M. Nitta, B. H. Zhelyazkova, C. J. Davidson, S. Akhavanfard, D. P. Cahill, K. D. Aldape, R. A. Betensky, D. N. Louis and A. J. Iafrate, *Cancer Cell*, 2011, 20, 810-817.
27. N. J. Szerlip, A. Pedraza, D. Chakravarty, M. Azim, J. McGuire, Y. Fang, T. Ozawa, E. C. Holland, J. T. Huse, S. Jhanwar, M. A. Leversha, T. Mikkelsen and C. W. Brennan, *Proc Natl Acad Sci U S A*, 2012, 109, 3041-3046.
28. K. Harada, T. Nishizaki, S. Ozaki, H. Kubota, H. Ito and K. Sasaki, *Cancer Res*, 1998, 58, 4694-4700.
29. V. Jung, B. F. Romeike, W. Henn, W. Feiden, J. R. Moringlane, K. D. Zang and S. Urbschat, *J Neuropathol Exp Neurol*, 1999, 58, 993-999.

30. P. J. Gardina, K. C. Lo, W. Lee, J. K. Cowell and Y. Turpaz, *BMC Genomics*, 2008, 9, 489.
31. S. Nobusawa, J. Lachuer, A. Wierinckx, Y. H. Kim, J. Huang, C. Legras, P. Kleihues and H. Ohgaki, *Brain Pathol*, 2010, 20, 936-944.
32. W. K. Yung, J. R. Shapiro and W. R. Shapiro, *Cancer Res*, 1982, 42, 992-998.
33. A. Besse, J. Sana, P. Fadrus and O. Slaby, *Tumour Biology : The Journal of the International Society for Oncodevelopmental Biology and Medicine*, 2013, DOI: 10.1007/s13277-013-0772-5.
34. K. J. Hatanpaa, S. Burma, D. Zhao and A. A. Habib, *Neoplasia*, 2010, 12, 675-684.
35. A. A. Khalil, M. J. Jameson, W. C. Broaddus, P. S. Lin and T. D. Chung, *Brain Tumor Pathology*, 2013, 30, 73-83.
36. S. Osuka, O. Sampetean, T. Shimizu, I. Saga, N. Onishi, E. Sugihara, J. Okubo, S. Fujita, S. Takano, A. Matsumura and H. Saya, *Stem Cells*, 2012, 31, 627-640.
37. H. F. Li, J. S. Kim and T. Waldman, *Radiation Oncology*, 2009, 4, 43.
38. S. E. Golding, R. N. Morgan, B. R. Adams, A. J. Hawkins, L. F. Povirk and K. Valerie, *Cancer Biology & Therapy*, 2009, 8, 730-738.
39. E. Chautard, G. Loubeau, A. Tchirkov, J. Chassagne, C. Vermot-Desroches, L. Morel and P. Verrelle, *Neuro-Oncology*, 2010, 12, 434-443.
40. J. Wang, T. P. Wakeman, J. D. Lathia, A. B. Hjelmeland, X. F. Wang, R. R. White, J. N. Rich and B. A. Sullenger, *Stem Cells*, 2010, 28, 17-28.
41. Y. Kim, K. H. Kim, J. Lee, Y. A. Lee, M. Kim, S. J. Lee, K. Park, H. Yang, J. Jin, K. M. Joo, J. Lee and D. H. Nam, *Laboratory Investigation; a Journal of Technical Methods and Pathology*, 2012, 92, 466-473.
42. P. K. Sharma and R. Varshney, *Free Radical Research*, 2012, 46, 1446-1457.
43. M. D. Naidu, J. M. Mason, R. V. Pica, H. Fung and L. A. Pena, *Journal of Radiation Research*, 2010, 51, 393-404.
44. Y. C. Lim, T. L. Roberts, B. W. Day, A. Harding, S. Kozlov, A. W. Kijas, K. S. Ensbey, D. G. Walker and M. F. Lavin, *Molecular Cancer Therapeutics*, 2012, 11, 1863-1872.
45. M. E. Hardee, A. E. Marciscano, C. M. Medina-Ramirez, D. Zagzag, A. Narayana, S. M. Lonning and M. H. Barcellos-Hoff, *Cancer Res*, 2012, 72, 4119-4129.
46. M. Jamal, B. H. Rath, P. S. Tsang, K. Camphausen and P. J. Tofilon, *Neoplasia*, 2012, 14, 150-158.
47. L. Yang, C. Lin, L. Wang, H. Guo and X. Wang, *Experimental Cell Research*, 2012, 318, 2417-2426.
48. A. Brondani Da Rocha, A. Regner, I. Grivicich, D. Pretto Schunemann, C. Diel, G. Kovaleski, C. Brunetto De Farias, E. Mondadori, L. Almeida, A. Braga Filho and G. Schwartzmann, *International Journal of Oncology*, 2004, 25, 777-785.
49. C. A. Fedrigo, I. Grivicich, D. P. Schunemann, I. M. Chemale, D. dos Santos, T. Jacovas, P. S. Boschetti, G. P. Jotz, A. Braga Filho and A. B. da Rocha, *Radiation Oncology*, 2011, 6, 156.
50. B. J. Denny, R. T. Wheelhouse, M. F. Stevens, L. L. Tsang and J. A. Slack, *Biochemistry*, 1994, 33, 9045-9051.
51. B. M. Alexander, N. Pinnell, P. Y. Wen and A. D'Andrea, *Journal of Neuro-Oncology*, 2012, 107, 463-477.
52. T. C. Johannessen and R. Bjerkvig, *Expert Review of Anticancer Therapy*, 2012, 12, 635-642.
53. C. Hunter, R. Smith, D. P. Cahill, P. Stephens, C. Stevens, J. Teague, C. Greenman, S. Edkins, G. Bignell, H. Davies, S. O'Meara, A. Parker, T. Avis, S. Barthorpe, L. Brackenbury, G. Buck, A. Butler, J. Clements, J. Cole, E. Dicks, S. Forbes, M. Gorton, K. Gray, K. Halliday, R. Harrison, K. Hills, J. Hinton, A. Jenkinson, D. Jones, V. Kosmidou, R. Laman, R. Lugg, A. Menzies, J. Perry, R. Petty, K. Raine, D. Richardson, R. Shepherd, A. Small, H. Solomon, C. Tofts, J. Varian, S. West, S. Widaa, A. Yates, D. F. Easton, G.

- Riggins, J. E. Roy, K. K. Levine, W. Mueller, T. T. Batchelor, D. N. Louis, M. R. Stratton, P. A. Futreal and R. Wooster, *Cancer Res*, 2006, 66, 3987-3991.
54. S. Yip, J. Miao, D. P. Cahill, A. J. Iafrate, K. Aldape, C. L. Nutt and D. N. Louis, *Clinical Cancer Research : an Official Journal of the American Association for Cancer Research*, 2009, 15, 4622-4629.
55. J. Felsberg, N. Thon, S. Eigenbrod, B. Hentschel, M. C. Sabel, M. Westphal, G. Schackert, F. W. Kreth, T. Pietsch, M. Loffler, M. Weller, G. Reifenberger, J. C. Tonn and N. German Glioma, *International Journal of Cancer. Journal international du cancer*, 2011, 129, 659-670.
56. A. M. Stark, A. Doukas, H. H. Hugo and H. M. Mehdorn, *Neurological Research*, 2010, 32, 816-820.
57. J. H. Sampson, A. B. Heimberger, G. E. Archer, K. D. Aldape, A. H. Friedman, H. S. Friedman, M. R. Gilbert, J. E. Herndon, 2nd, R. E. McLendon, D. A. Mitchell, D. A. Reardon, R. Sawaya, R. J. Schmittling, W. Shi, J. J. Vredenburgh and D. D. Bigner, *Journal of Clinical Oncology : Official Journal of the American Society of Clinical Oncology*, 2010, 28, 4722-4729.
58. A. J. Wong, J. M. Ruppert, S. H. Bigner, C. H. Grzeschik, P. A. Humphrey, D. S. Bigner and B. Vogelstein, *Proc Natl Acad Sci U S A*, 1992, 89, 2965-2969.
59. R. Nishikawa, T. Sugiyama, Y. Narita, F. Furnari, W. K. Cavenee and M. Matsutani, *Brain Tumor Pathology*, 2004, 21, 53-56.
60. M. M. Inda, R. Bonavia, A. Mukasa, Y. Narita, D. W. Sah, S. Vandenberg, C. Brennan, T. G. Johns, R. Bachoo, P. Hadwiger, P. Tan, R. A. Depinho, W. Cavenee and F. Furnari, *Genes Dev*, 2010, 24, 1731-1745.
61. M. Hermanson, K. Funo, M. Hartman, L. Claesson-Welsh, C. H. Heldin, B. Westermark and M. Nister, *Cancer Res*, 1992, 52, 3213-3219.
62. K. Nabeshima, Y. Shimao, S. Sato, H. Kataoka, T. Moriyama, H. Kawano, S. Wakisaka and M. Koono, *Histopathology*, 1997, 31, 436-443.
63. S. E. Little, S. Popov, A. Jury, D. A. Bax, L. Doey, S. Al-Sarraj, J. M. Jurgensmeier and C. Jones, *Cancer Res*, 2012, 72, 1614-1620.
64. N. Ishii, M. Tada, M. F. Hamou, R. C. Janzer, K. Meagher-Villemure, O. D. Wiestler, N. Tribolet and E. G. Van Meir, *Oncogene*, 1999, 18, 5870-5878.
65. K. Koga, T. Todaka, M. Morioka, J. Hamada, Y. Kai, S. Yano, A. Okamura, N. Takakura, T. Suda and Y. Ushio, *Cancer Res*, 2001, 61, 6248-6254.
66. L. Bello, M. Francolini, P. Marthyn, J. Zhang, R. S. Carroll, D. C. Nikas, J. F. Strasser, R. Villani, D. A. Cheresch and P. M. Black, *Neurosurgery*, 2001, 49, 380-389; discussion 390.
67. M. E. Hegi, L. Liu, J. G. Herman, R. Stupp, W. Wick, M. Weller, M. P. Mehta and M. R. Gilbert, *Journal of Clinical Oncology : Official Journal of the American Society of Clinical Oncology*, 2008, 26, 4189-4199.
68. M. Castedo, A. Coquelle, I. Vitale, S. Vivet, S. Mouhamad, S. Viaud, L. Zitvogel and G. Kroemer, *Annals of the New York Academy of Sciences*, 2006, 1090, 35-49.
69. Q. Wang, P. C. Wu, D. Z. Dong, I. Ivanova, E. Chu, S. Zeliadt, H. Vesselle and D. Y. Wu, *International Journal of Cancer. Journal International du Cancer*, 2012, DOI: 10.1002/ijc.27810.
70. P. Balsas, P. Galan-Malo, I. Marzo and J. Naval, *Leukemia Research*, 2012, 36, 212-218.
71. C. Lagadec, E. Vlashi, L. Della Donna, C. Dekmezian and F. Pajonk, *Stem Cells*, 2012, 30, 833-844.
72. S. Sharma, J. Y. Zeng, C. M. Zhuang, Y. Q. Zhou, H. P. Yao, X. Hu, R. Zhang and M. H. Wang, *Molecular Cancer Therapeutics*, 2013, 12, 725-736.
73. I. Vitale, L. Galluzzi, S. Vivet, L. Nanty, P. Dessen, L. Senovilla, K. A. Olaussen, V. Lazar, M. Prudhomme, R. M. Golsteyn, M. Castedo and G. Kroemer, *PLoS One*, 2007, 2, e1337.
74. S. Rello-Varona, I. Vitale, O. Kepp, L. Senovilla, M. Jemaa, D. Metivier, M. Castedo and G. Kroemer, *Cell Cycle*, 2009, 8, 1030-1035.

75. A. J. Lee, R. Roylance, J. Sander, P. Gorman, D. Endesfelder, M. Kschischo, N. P. Jones, P. East, B. Nicke, S. Spassieva, L. M. Obeid, N. J. Birkbak, Z. Szallasi, N. C. McKnight, A. J. Rowan, V. Speirs, A. M. Hanby, J. Downward, S. A. Tooze and C. Swanton, *The Journal of Pathology*, 2012, 226, 482-494.
76. M. Roh, R. van der Meer and S. A. Abdulkadir, *Journal of Cellular Physiology*, 2012, 227, 801-812.
77. M. Marxer, C. E. Foucar, W. Y. Man, Y. Chen, H. T. Ma and R. Y. Poon, *Cell Cycle*, 2012, 11, 2567-2577.
78. D. N. Louis, H. Ohgaki, O. D. Wiestler, W. K. Cavenee, P. C. Burger, A. Jouvet, B. W. Scheithauer and P. Kleihues, *Acta Neuropathol*, 2007, 114, 97-109.
79. L. P. Deleyrolle and B. A. Reynolds, *Methods in Molecular Biology*, 2009, 549, 91-101.
80. R. Galli, E. Binda, U. Orfanelli, B. Cipelletti, A. Gritti, S. De Vitis, R. Fiocco, C. Foroni, F. Dimeco and A. Vescovi, *Cancer Res*, 2004, 64, 7011-7021.
81. J. Lee, S. Kotliarova, Y. Kotliarov, A. Li, Q. Su, N. M. Donin, S. Pastorino, B. W. Purow, N. Christopher, W. Zhang, J. K. Park and H. A. Fine, *Cancer Cell*, 2006, 9, 391-403.
82. D. R. Laks, M. Masterman-Smith, K. Visnyei, B. Angenieux, N. M. Orozco, I. Foran, W. H. Yong, H. V. Vinters, L. M. Liao, J. A. Lazareff, P. S. Mischel, T. F. Cloughesy, S. Horvath and H. I. Kornblum, *Stem Cells*, 2009, 27, 980-987.
83. E. H. Panosyan, D. R. Laks, M. Masterman-Smith, J. Mottahedeh, W. H. Yong, T. F. Cloughesy, J. A. Lazareff, P. S. Mischel, T. B. Moore and H. I. Kornblum, *Pediatric Blood & Cancer*, 2010, 55, 644-651.
84. S. J. Jones, A. J. Dicker, A. L. Dahler and N. A. Saunders, *The Journal of Investigative Dermatology*, 1997, 109, 187-193.
85. L. P. Deleyrolle, A. Harding, K. Cato, F. A. Siebzehnrubl, M. Rahman, H. Azari, S. Olson, B. Gabrielli, G. Osborne, A. Vescovi and B. A. Reynolds, *Brain : a Journal of Neurology*, 2011, 134, 1331-1343.
86. M. Serra, M. Tarkkanen, N. Baldini, K. Scotlandi, M. Sarti, D. Maurici, M. C. Manara, S. Benini, P. Bacchini, S. Knuutila and P. Picci, *Modern Pathology*, 2001, 14, 710.
87. T. Mosmann, *J Immunol Methods*, 1983, 65, 55-63.
88. S. A. Louis and B. A. Reynolds, *Methods in Molecular Biology*, 2005, 290, 265-280.
89. E. M. Torres, T. Sokolsky, C. M. Tucker, L. Y. Chan, M. Boselli, M. J. Dunham and A. Amon, *Science*, 2007, 317, 916-924.
90. G. Rancati, N. Pavelka, B. Fleharty, A. Noll, R. Trimble, K. Walton, A. Perera, K. Staehling-Hampton, C. W. Seidel and R. Li, *Cell*, 2008, 135, 879-893.
91. B. R. Williams, V. R. Prabhu, K. E. Hunter, C. M. Glazier, C. A. Whittaker, D. E. Housman and A. Amon, *Science*, 2008, 322, 703-709.
92. G. Gentric, S. Celton-Morizur and C. Desdouets, *Clinics and Research in Hepatology and Gastroenterology*, 2012, 36, 29-34.
93. D. Hanahan and R. A. Weinberg, *Cell*, 2011, 144, 646-674.
94. S. Polakova, C. Blume, J. A. Zarate, M. Mentel, D. Jorck-Ramberg, J. Stenderup and J. Piskur, *Proc Natl Acad Sci U S A*, 2009, 106, 2688-2693.
95. N. Pavelka, G. Rancati, J. Zhu, W. D. Bradford, A. Saraf, L. Florens, B. W. Sanderson, G. L. Hattem and R. Li, *Nature*, 2010, 468, 321-325.
96. G. Chen, W. D. Bradford, C. W. Seidel and R. Li, *Nature*, 2012, 482, 246-250.
97. J. Bullwinkel, B. Baron-Luhr, A. Ludemann, C. Wohlenberg, J. Gerdes and T. Scholzen, *Journal of Cellular Physiology*, 2006, 206, 624-635.
98. K. Kontzoglou, V. Palla, G. Karaolani, I. Karaiskos, I. Alexiou, I. Pateras, K. Konstantoudakis and M. Stamatakis, *Oncology*, 2013, 84, 219-225.
99. N. Kachroo and V. J. Gnanapragasam, *Journal of Cancer Research and Clinical Oncology*, 2013, 139, 1-24.
100. S. J. Ohsie, G. P. Sarantopoulos, A. J. Cochran and S. W. Binder, *Journal of Cutaneous Pathology*, 2008, 35, 433-444.

101. A. Pich, L. Chiusa and R. Navone, *Annals of Oncology : Official Journal of the European Society for Medical Oncology / ESMO*, 2004, 15, 1319-1329.
102. M. H. Faria, B. P. Goncalves, R. M. do Patrocinio, M. O. de Moraes-Filho and S. H. Rabenhorst, *Neuropathology : Official Journal of the Japanese Society of Neuropathology*, 2006, 26, 519-527.
103. F. Kayaselcuk, S. Zorludemir, D. Gumurduhu, H. Zeren and T. Erman, *Journal of Neuro-Oncology*, 2002, 57, 115-121.
104. C. J. Sherr and F. McCormick, *Cancer Cell*, 2002, 2, 103-112.
105. A. B. Lyons, *J Immunol Methods*, 2000, 243, 147-154.
106. A. B. Lyons, S. J. Blake and K. V. Doherty, *Current Protocols in Cytometry*, 2013, Chapter 9, Unit9 11.
107. S. M. Graham, H. G. Jorgensen, E. Allan, C. Pearson, M. J. Alcorn, L. Richmond and T. L. Holyoake, *Blood*, 2002, 99, 319-325.
108. K. Krishnamurthy, G. Wang, D. Rokhfeld and E. Bieberich, *Breast Cancer Research : BCR*, 2008, 10, R106.
109. J. L. Dembinski and S. Krauss, *Clinical & Experimental Metastasis*, 2009, 26, 611-623.
110. S. Pece, D. Tosoni, S. Confalonieri, G. Mazzarol, M. Vecchi, S. Ronzoni, L. Bernard, G. Viale, P. G. Pelicci and P. P. Di Fiore, *Cell*, 2010, 140, 62-73.
111. A. Roesch, M. Fukunaga-Kalabis, E. C. Schmidt, S. E. Zabierowski, P. A. Brafford, A. Vultur, D. Basu, P. Gimotty, T. Vogt and M. Herlyn, *Cell*, 2010, 141, 583-594.
112. E. M. Torres, N. Dephoure, A. Panneerselvam, C. M. Tucker, C. A. Whittaker, S. P. Gygi, M. J. Dunham and A. Amon, *Cell*, 2010, 143, 71-83.
113. T. R. Gregory, *Biological Reviews of the Cambridge Philosophical Society*, 2001, 76, 65-101.
114. D. A. Petrov, *Theoretical Population Biology*, 2002, 61, 531-544.
115. T. Cavalier-Smith, *Annals of Botany*, 2005, 95, 147-175.
116. Y. H. Chan and W. F. Marshall, *Organogenesis*, 2010, 6, 88-96.
117. F. R. Neumann and P. Nurse, *The Journal of Cell Biology*, 2007, 179, 593-600.
118. P. Jorgensen, N. P. Edgington, B. L. Schneider, I. Rupes, M. Tyers and B. Futcher, *Molecular Biology of the Cell*, 2007, 18, 3523-3532.
119. H. Dolznig, F. Grebien, T. Sauer, H. Beug and E. W. Mullner, *Nature Cell Biology*, 2004, 6, 899-905.
120. R. Kafri, J. Levy, M. B. Ginzberg, S. Oh, G. Lahav and M. W. Kirschner, *Nature*, 2013, 494, 480-483.
121. R. A. Gatenby and R. J. Gillies, *The International Journal of Biochemistry & Cell Biology*, 2007, 39, 1358-1366.
122. M. Jain, R. Nilsson, S. Sharma, N. Madhusudhan, T. Kitami, A. L. Souza, R. Kafri, M. W. Kirschner, C. B. Clish and V. K. Mootha, *Science*, 2012, 336, 1040-1044.
123. R. L. Aft, F. W. Zhang and D. Gius, *Br J Cancer*, 2002, 87, 805-812.
124. S. Gupta, A. Farooque, J. S. Adhikari, S. Singh and B. S. Dwarakanath, *Journal of Cancer Research and Therapeutics*, 2009, 5 Suppl 1, S16-20.
125. F. Zhang and R. L. Aft, *Journal of Cancer Research and Therapeutics*, 2009, 5 Suppl 1, S41-43.
126. V. K. Kalia, S. Prabhakara and V. Narayanan, *Journal of Cancer Research and Therapeutics*, 2009, 5 Suppl 1, S57-60.
127. R. Beroukhi, C. H. Mermel, D. Porter, G. Wei, S. Raychaudhuri, J. Donovan, J. Barretina, J. S. Boehm, J. Dobson, M. Urashima, K. T. Mc Henry, R. M. Pinchback, A. H. Ligon, Y. J. Cho, L. Haery, H. Greulich, M. Reich, W. Winckler, M. S. Lawrence, B. A. Weir, K. E. Tanaka, D. Y. Chiang, A. J. Bass, A. Loo, C. Hoffman, J. Prensner, T. Liefeld, Q. Gao, D. Yecies, S. Signoretti, E. Maher, F. J. Kaye, H. Sasaki, J. E. Tepper, J. A. Fletcher, J. Taberner, J. Baselga, M. S. Tsao, F. Demicheli, M. A. Rubin, P. A. Janne, M. J. Daly, C. Nucera, R. L. Levine, B. L. Ebert, S. Gabriel, A. K. Rustgi, C. R. Antonescu, M. Ladanyi,

- A. Letai, L. A. Garraway, M. Loda, D. G. Beer, L. D. True, A. Okamoto, S. L. Pomeroy, S. Singer, T. R. Golub, E. S. Lander, G. Getz, W. R. Sellers and M. Meyerson, *Nature*, 2010, 463, 899-905.
128. T. Fujiwara, M. Bandi, M. Nitta, E. V. Ivanova, R. T. Bronson and D. Pellman, *Nature*, 2005, 437, 1043-1047.
129. A. Castillo, H. C. Morse, 3rd, V. L. Godfrey, R. Naeem and M. J. Justice, *Cancer Res*, 2007, 67, 10138-10147.
130. T. Davoli and T. de Lange, *Cancer Cell*, 2012, 21, 765-776.
131. L. Zheng, H. Dai, M. Zhou, X. Li, C. Liu, Z. Guo, X. Wu, J. Wu, C. Wang, J. Zhong, Q. Huang, J. Garcia-Aguilar, G. P. Pfeifer and B. Shen, *Nat Commun*, 2012, 3, 815.
132. T. Boveri, *Neu Folge*, 1902, 35, 67-90.
133. T. D. Randall and I. L. Weissman, *Blood*, 1997, 89, 3596-3606.
134. A. Wilson, E. Laurenti, G. Oser, R. C. van der Wath, W. Blanco-Bose, M. Jaworski, S. Offner, C. F. Dunant, L. Eshkind, E. Bockamp, P. Lio, H. R. Macdonald and A. Trumpp, *Cell*, 2008, 135, 1118-1129.
135. M. A. Essers, S. Offner, W. E. Blanco-Bose, Z. Waibler, U. Kalinke, M. A. Duchosal and A. Trumpp, *Nature*, 2009, 458, 904-908.
136. T. A. Davis, O. Mungunsukh, S. Zins, R. M. Day and M. R. Landauer, *International Journal of Radiation Biology*, 2008, 84, 713-726.
137. S. M. Johnson, C. D. Torrice, J. F. Bell, K. B. Monahan, Q. Jiang, Y. Wang, M. R. Ramsey, J. Jin, K. K. Wong, L. Su, D. Zhou and N. E. Sharpless, *J Clin Invest*, 2010, 120, 2528-2536.
138. C. E. Forristal, I. G. Winkler, B. Nowlan, V. Barbier, G. Walkinshaw and J. P. Levesque, *Blood*, 2013, 121, 759-769.
139. M. A. Shah and G. K. Schwartz, *Clinical Cancer Research : an Official Journal of the American Association for Cancer Research*, 2001, 7, 2168-2181.
140. M. Schmidt, Y. Lu, J. M. Parant, G. Lozano, G. Bacher, T. Beckers and Z. Fan, *Molecular Pharmacology*, 2001, 60, 900-906.
141. G. N. Naumov, J. L. Townson, I. C. MacDonald, S. M. Wilson, V. H. Bramwell, A. C. Groom and A. F. Chambers, *Breast Cancer Research and Treatment*, 2003, 82, 199-206.
142. C. M. Fillmore and C. Kuperwasser, *Breast Cancer Research : BCR*, 2008, 10, R25.
143. A. P. Kusumbe and S. A. Bapat, *Cancer Res*, 2009, 69, 9245-9253.
144. N. Moore, J. Houghton and S. Lyle, *Stem Cells and Development*, 2012, 21, 1822-1830.
145. Y. Chen, D. Li, D. Wang, X. Liu, N. Yin, Y. Song, S. H. Lu, Z. Ju and Q. Zhan, *Journal of Cellular Biochemistry*, 2012, 113, 3643-3652.
146. J. Chen, Y. Li, T. S. Yu, R. M. McKay, D. K. Burns, S. G. Kernie and L. F. Parada, *Nature*, 2012, 488, 522-526.
147. S. Kobayashi, H. Yamada-Okabe, M. Suzuki, O. Natori, A. Kato, K. Matsubara, Y. Jau Chen, M. Yamazaki, S. Funahashi, K. Yoshida, E. Hashimoto, Y. Watanabe, H. Mutoh, M. Ashihara, C. Kato, T. Watanabe, T. Yoshikubo, N. Tamaoki, T. Ochiya, M. Kuroda, A. J. Levine and T. Yamazaki, *Stem Cells*, 2012, 30, 2631-2644.
148. A. Kreso, C. A. O'Brien, P. van Galen, O. I. Gan, F. Notta, A. M. Brown, K. Ng, J. Ma, E. Wienholds, C. Dunant, A. Pollett, S. Gallinger, J. McPherson, C. G. Mullighan, D. Shibata and J. E. Dick, *Science*, 2013, 339, 543-548.
149. J. J. Turner, J. C. Ewald and J. M. Skotheim, *Current Biology : CB*, 2012, 22, R350-359.
150. G. C. Johnston, J. R. Pringle and L. H. Hartwell, *Experimental Cell Research*, 1977, 105, 79-98.
151. C. Martin-Castellanos, M. A. Blanco, J. M. de Prada and S. Moreno, *Molecular Biology of the Cell*, 2000, 11, 543-554.
152. Y. Hirose, M. S. Berger and R. O. Pieper, *Cancer Res*, 2001, 61, 5843-5849.
153. A. Jinno-Oue, N. Shimizu, N. Hamada, S. Wada, A. Tanaka, M. Shinagawa, T. Ohtsuki, T. Mori, M. N. Saha, A. S. Hoque, S. Islam, K. Kogure, T. Funayama, Y. Kobayashi and H.

- Hoshino, *International Journal of Radiation Oncology, Biology, Physics*, 2010, 76, 229-241.
154. A. V. Knizhnik, W. P. Roos, T. Nikolova, S. Quiros, K. H. Tomaszowski, M. Christmann and B. Kaina, *PLoS One*, 2013, 8, e55665.
 155. T. Galitski, A. J. Saldanha, C. A. Styles, E. S. Lander and G. R. Fink, *Science*, 1999, 285, 251-254.
 156. A. Selmecki, A. Forche and J. Berman, *Eukaryot Cell*, 2010, 9, 991-1008.
 157. J. W. Kronstad, R. Attarian, B. Cadieux, J. Choi, C. A. D'Souza, E. J. Griffiths, J. M. Geddes, G. Hu, W. H. Jung, M. Kretschmer, S. Saikia and J. Wang, *Nature Reviews. Microbiology*, 2011, 9, 193-203.
 158. S. F. Elena, P. Carrasco, J. A. Daros and R. Sanjuan, *EMBO Reports*, 2006, 7, 168-173.
 159. T. Davoli and T. de Lange, *Annual Review of Cell and Developmental Biology*, 2011, 27, 585-610.
 160. S. J. Pfau and A. Amon, *EMBO Reports*, 2012, 13, 515-527.
 161. J. Erenpreisa and M. S. Cragg, *Cancer Cell International*, 2013, 13, 92.
 162. S. E. Shackney, C. A. Smith, B. W. Miller, D. R. Burholt, K. Murtha, H. R. Giles, D. M. Ketterer and A. A. Pollice, *Cancer Res*, 1989, 49, 3344-3354.
 163. Y. C. Tang, B. R. Williams, J. J. Siegel and A. Amon, *Cell*, 2011.

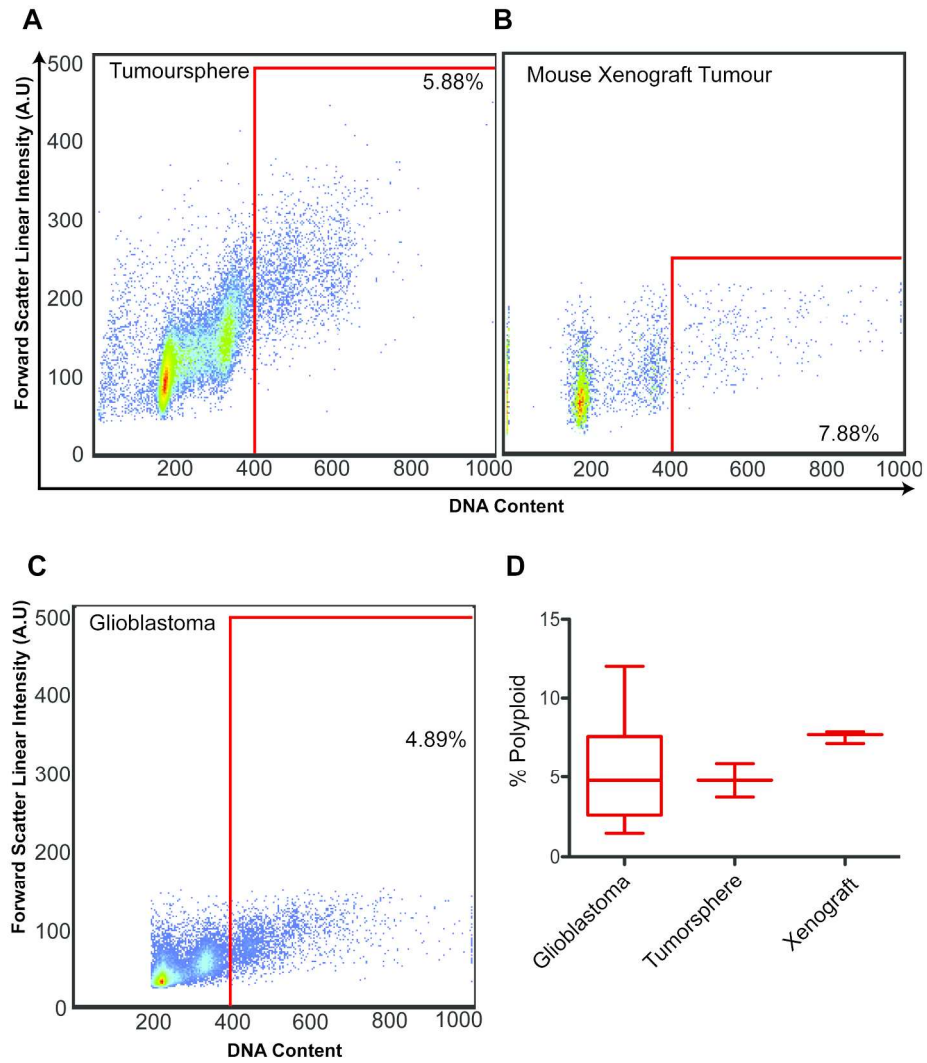


Figure 1

209x272mm (300 x 300 DPI)

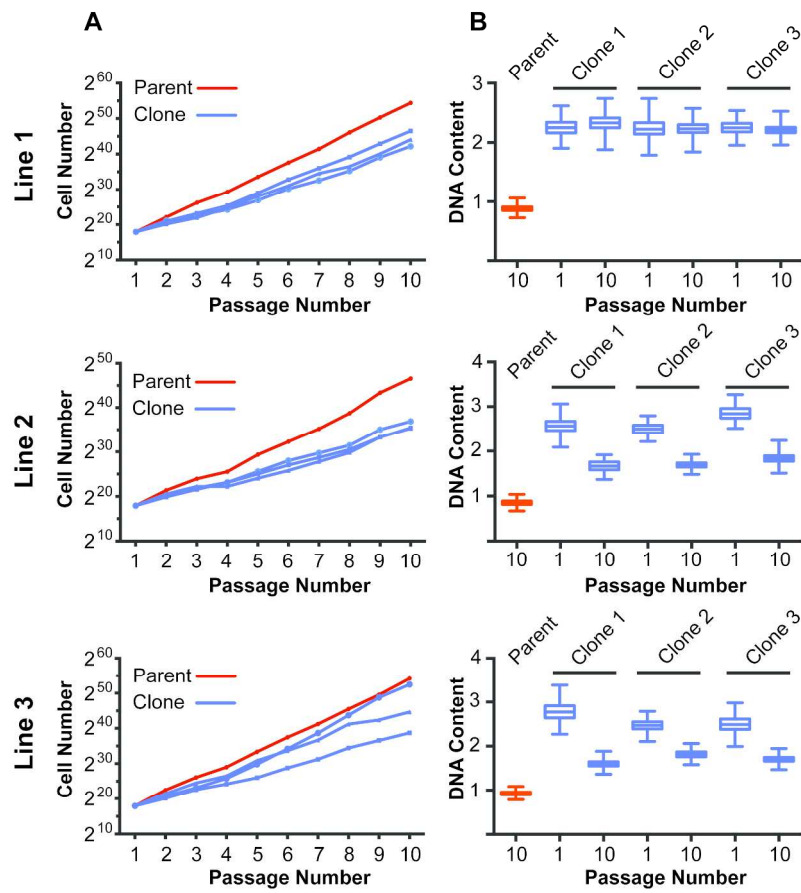


Figure 2

210x297mm (300 x 300 DPI)

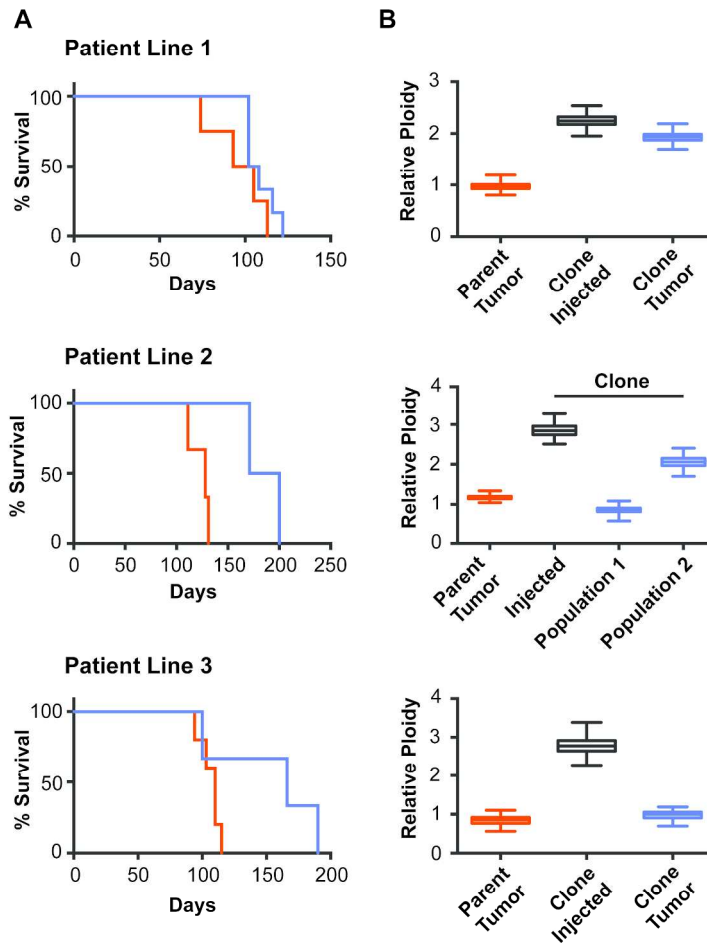


Figure 3

210x297mm (300 x 300 DPI)

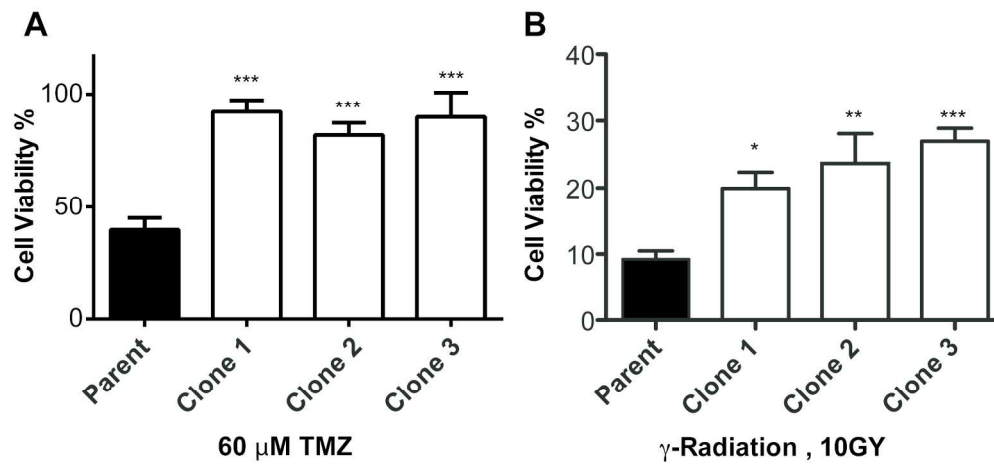


Figure 4

190x127mm (300 x 300 DPI)

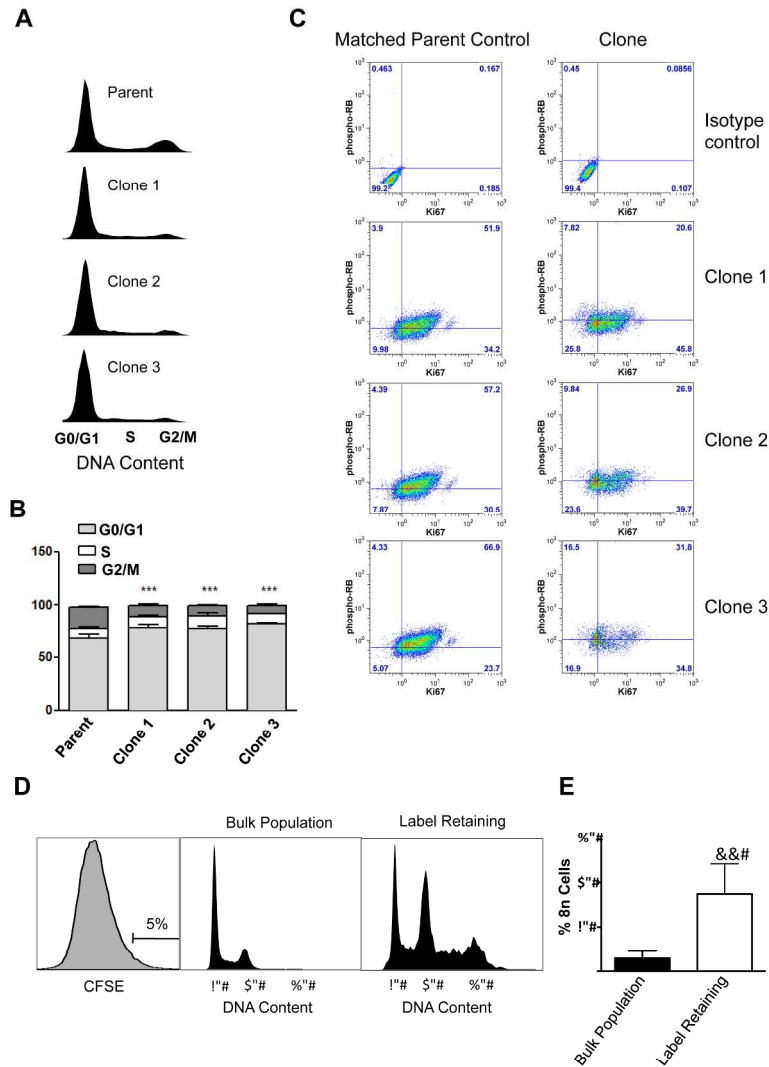


Figure 5

219x268mm (300 x 300 DPI)

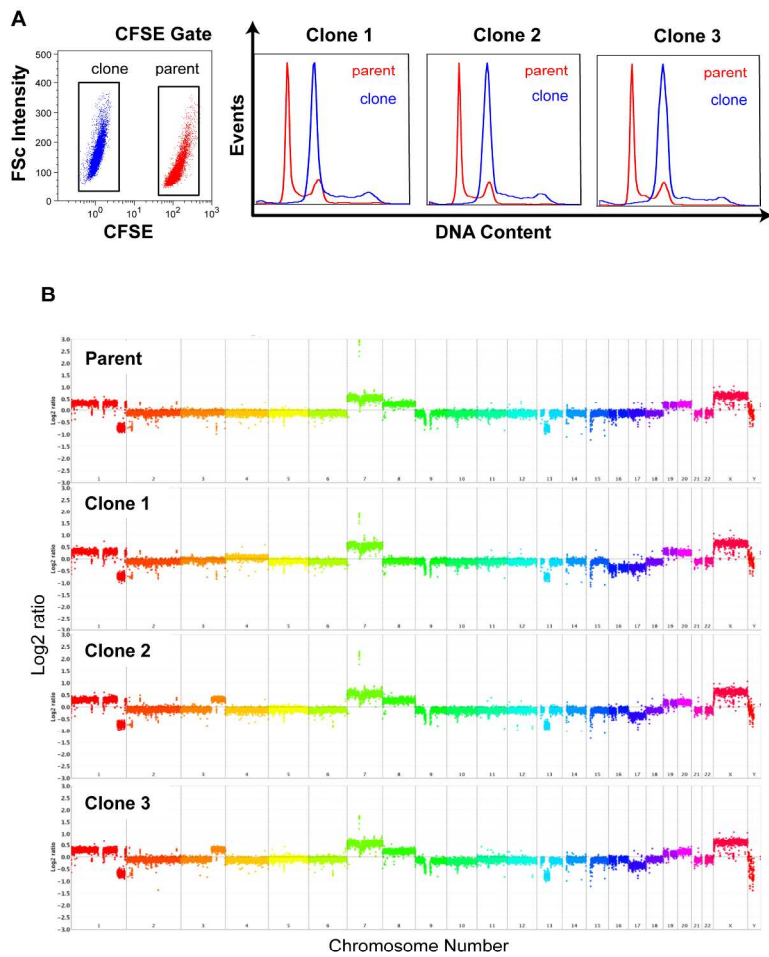


Figure 6

210x270mm (300 x 300 DPI)

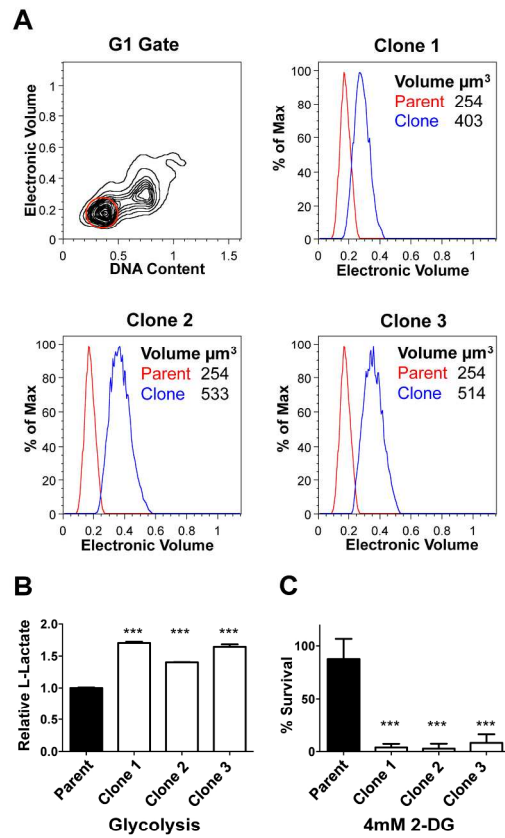


Figure 7

185x268mm (300 x 300 DPI)